

# Regime Transition of the North Atlantic Oscillation and the Extreme Cold Event over Europe in January–February 2012

DEHAI LUO

*Regional Climate-Environment for Temperate East Asia, Institute of Atmospheric Physics, Chinese Academy of Science, Beijing, China*

YAO YAO

*Regional Climate-Environment for Temperate East Asia, Institute of Atmospheric Physics, Chinese Academy of Science, Beijing, and Physical Oceanography Laboratory, College of Physical and Environmental Oceanography, Ocean University of China, Qingdao, China*

STEVEN B. FELDSTEIN

*Department of Meteorology, The Pennsylvania State University, University Park, Pennsylvania*

(Manuscript received 20 July 2013, in final form 26 July 2014)

## ABSTRACT

In this paper, large-scale aspects for the onset of the extreme cold European weather event in January–February 2012 are investigated. It is shown that the outbreak of this extreme cold weather event may be attributed to the transition from a positive North Atlantic Oscillation (NAO<sup>+</sup>) event to a long-lasting blocking event over the eastern Atlantic and western Europe (hereafter ENAO<sup>-</sup>). A persistent decline of the surface air temperature (SAT) is seen over all of Europe during the long-lived ENAO<sup>-</sup> event, while the main region of enhanced precipitation is located over southern Europe and part of central Europe, in association with the presence of a persistent double storm track: one over the Norwegian and Barents Seas and the other over southern Europe.

The NAO<sup>+</sup> to NAO<sup>-</sup> transition events are divided into NAO<sup>+</sup> to ENAO<sup>-</sup> and NAO<sup>+</sup> to WNAO<sup>-</sup> transition events [ENAO<sup>-</sup> (WNAO<sup>-</sup>) events correspond to eastward- (westward-) displaced NAO<sup>-</sup> events whose positive center is defined to be located to the east (west) of 10°W], and a statistical analysis of the NAO<sup>+</sup> to ENAO<sup>-</sup> transition events during 1978–2012 is performed. It is found that there has been a marked increase in the frequency of the NAO<sup>+</sup> to ENAO<sup>-</sup> transition events during the period 2005–12. Composites of SAT anomalies indicate that the marked decline of the SAT observed over much of Europe is primarily associated with NAO<sup>+</sup> to ENAO<sup>-</sup> transition events. Thus, NAO<sup>+</sup> to ENAO<sup>-</sup> transition events may be more favorable for the extreme cold events over Europe observed in recent winters than other types of NAO<sup>-</sup> events.

## 1. Introduction

Observations show that during January–February 2012, an extreme cold event occurred over the European continent. This event affected central and eastern Europe, and also parts of Asia, for the two-week period from 27 January to 10 February 2012, as reported by the

Tokyo climate center, Japan Meteorological Agency ([http://ds.data.jma.go.jp/tcc/tcc/news/Cold\\_Wave\\_over\\_the\\_Eurasian\\_Continent.pdf](http://ds.data.jma.go.jp/tcc/tcc/news/Cold_Wave_over_the_Eurasian_Continent.pdf)). The low temperature of  $-39.2^{\circ}\text{C}$  on 2 February in Finland was recorded and this cold event led to the deaths of several hundred people over several eastern European countries (<http://www.nipccreport.org/articles/2012/feb/15feb2012a3.html>).

In recent years, extreme cold events in winter were frequently observed over the Eurasian continent (Sillmann et al. 2011; Zhang et al. 2012) and their physical causes have attracted widespread interest among atmospheric scientists (Cattiaux et al. 2010; Seager et al. 2010; Wang

---

*Corresponding author address:* Dr. Dehai Luo, RCE-TEA, Institute of Atmospheric Physics, Chinese Academy of Science, P.O. Box 9804, West Beichen Rd., Beijing 100029, China.  
E-mail: ldh@mail.iap.ac.cn

et al. 2010; Buehler et al. 2011; De Vries et al. 2012). Many investigations have revealed that the cold events over European continent are not only related to the occurrence of Atlantic–European blocking events (Sillmann et al. 2011), but also to the phase of the North Atlantic Oscillation (NAO; Cattiaux et al. 2010; Seager et al. 2010).

Several studies indicated that the phase of the NAO event, which occurs with a time scale of 10–20 days, can significantly influence the winter weather and climate over Europe and Asia (Hurrell 1995; Werner et al. 2000; Yiou and Nogaj 2004; Scaife et al. 2008; Croci-Maspoli and Davies 2009; Cattiaux et al. 2010; Seager et al. 2010; Wang et al. 2010). The positive phase of the NAO (NAO<sup>+</sup>) is associated with an enhanced southwest–northeast-oriented North Atlantic jet stream and tends to correspond to positive temperature anomalies in northern Europe and negative temperature anomalies over central and southern Europe (Hurrell 1995; Hurrell and van Loon 1997; Vicente-Serrano and López-Moreno 2008). For the negative NAO phase (NAO<sup>-</sup>), negative temperature anomalies are seen over central and northern Europe (Buehler et al. 2011). Sillmann et al. (2011) also found that North Atlantic blocking conditions can explain in part the occurrence of anomalous cold winter temperatures over Europe, although blocking events occurring over the western North Atlantic seem to have less influence on temperatures in Europe than do blocking events closer to the continent. In a case study, Croci-Maspoli and Davies (2009) found that the anomalously cold European winter of 2005/06 is closely related to the occurrence of Atlantic blocking located west of the continent. Cattiaux et al. (2010), Seager et al. (2010), and Wang et al. (2010) attributed the anomalous cold winter of 2009/10 to the extreme negative NAO and Arctic Oscillation (AO), along with the occurrence of an El Niño event.

To compare NAO events observed during the 2011/12 and 2009/10 winters, we show the time series of the daily NAO index and domain-averaged surface air temperature (SAT) anomaly over the European continent (30°–75°N, 10°W–60°E) during the 2009/10 and 2011/12 winters in Figs. 1a and 1b, respectively. It is seen that the daily NAO index during the 2011/12 winter (November/March) is mostly positive, evidently different from that of the negative NAO index during the 2009/10 winter. However, a strong persistent negative SAT anomaly is seen over the European continent in January–February 2012 (Fig. 1b) although the NAO index during the 2011/12 winter is almost positive. Santos et al. (2013) noted anomalous warmth over northern Europe during the 2011/12 winter (see their Fig. 5). Further calculation shows that the 2011/12 winter is warmer than the 2009/10 winter because the winter mean SAT anomaly averaged

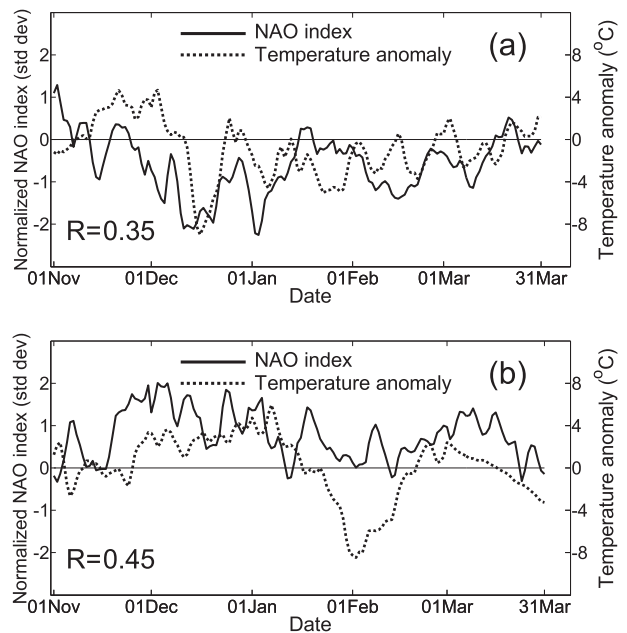


FIG. 1. Time series of the normalized daily NAO index (solid) and surface air temperature (SAT) anomaly (dashed) averaged over the European continent (30°–75°N, 10°W–60°E) during the (a) 2009/10 and (b) 2011/12 winters. The correlation coefficient between the normalized NAO index and regional-averaged SAT time series is indicated in (a) and (b). The daily temperature anomaly is defined as the daily temperature departure from the mean value for each particular day of the winter during 1978–2012, in which the seasonal cycle has been removed.

over the European continent is 0.1°C (0.3°C) for the 2011/12 winter and  $-0.9^{\circ}\text{C}$  ( $-1.9^{\circ}\text{C}$ ) for the 2009/10 winter for a winter mean from November to March (December to February). Even so, January–February 2012 is extremely cold (Fig. 1b) during a positive NAO. This implies that the variation of the SAT anomaly over Europe during the 2011/12 winter cannot be explained by the phase of the NAO. As we will see, the European SAT variation is more likely to be explained by the temporal variation of the NAO index. Thus, the different variations of the daily NAO index and SAT anomaly during the 2009/10 and 2011/12 winters suggest that the mechanisms governing the extreme cold weather event in January–February 2012 may be distinct from those of the 2009/10 winter, although the negative NAO phase corresponds generally to negative SAT anomalies over northern Europe (Cattiaux et al. 2010; Seager et al. 2010). In this paper, we will attempt to examine what particular type of large-scale pattern changes lead to the occurrence of the extreme cold European weather event in January–February 2012, and to provide an understanding of whether the large-scale characteristics of this recent cold air outbreak are similar to those of other recent wintertime cold air outbreaks over Europe.

Although many indices have been proposed to identify NAO events, in this paper, using a region-averaged NAO index defined by [Li and Wang \(2003\)](#), we show that there is a link between the extreme cold weather event over Europe in January–February 2012 and the transition from a  $\text{NAO}^+$  event to a long-lasting blocking event over the eastern Atlantic and western Europe. Because  $\text{NAO}^-$  events correspond to blocking events over Greenland and the North Atlantic ([Luo et al. 2007](#); [Woollings et al. 2008](#); [Davini et al. 2012](#)), it is reasonable to define blocking events over the North Atlantic and eastern Atlantic–European continent as the negative phase western NAO ( $\text{WNAO}^-$ ) and eastern NAO ( $\text{ENAO}^-$ ) events, respectively, to unify the  $\text{NAO}^-$  and eastern Atlantic–European blocking events into a single  $\text{NAO}^-$  system. This leads us to conveniently examine which type of  $\text{NAO}^-$  regimes contribute more importantly to extreme cold events over Europe.

The dynamical mechanisms leading to the occurrence of an  $\text{NAO}^+$  to  $\text{NAO}^-$  transition event have been examined in recent studies (e.g., [Luo et al. 2011](#); [Michel and Rivière 2011](#); [Luo and Cha 2012](#)). As revealed by [Luo and Cha \(2012\)](#) with a nonlinear multiscale interaction model, whether the  $\text{NAO}^+$  to  $\text{NAO}^-$  transition event can take place depends crucially on the strength of the mean zonal wind or jet stream over the North Atlantic prior to the NAO onset. When the mean zonal wind is relatively weak, the intensified block over the European continent that follows the  $\text{NAO}^+$  event moves far westward, entering the Atlantic basin and allowing for an  $\text{NAO}^+$  to  $\text{WNAO}^-$  transition event to occur (if Atlantic blocking event is defined as a  $\text{WNAO}^-$  event) ([Luo and Cha 2012](#)). However, when the mean zonal wind or jet stream is relatively strong, the retrograde movement of the European blocking pattern is suppressed and blocking always remains over the continent. In this case, the  $\text{NAO}^+$  to eastern Atlantic–European blocking regime transition takes place and is identified as an  $\text{NAO}^+$  to  $\text{ENAO}^-$  transition event (if eastern Atlantic–European blocking is defined as an  $\text{ENAO}^-$  event). [Santos et al. \(2013\)](#) noted that the Atlantic jet was stronger during the 2011/12 winter than during the 2009/10 winter. The stronger North Atlantic jet has a favorable condition for an  $\text{NAO}^+$  to  $\text{ENAO}^-$  transition event. In this paper, we will present an observational study to demonstrate that the  $\text{NAO}^+$  to  $\text{ENAO}^-$  transition event is more favorable for the occurrence of extreme cold European weather events as observed in January–February 2012 than other types of  $\text{NAO}^-$  regimes.

In the present observational study, a case analysis and composite analyses are performed. In our case study, we show that there is a link between the SAT variation and

a persistent  $\text{ENAO}^-$  pattern through a persistent splitting of the transient eddy energy within the storm track (defined as the maximum core of synoptic-scale eddy kinetic energy) over the Euro–Atlantic sector. This association can occur because the spatial structures of the regional temperature and precipitation anomalies are mostly determined by the spatial distribution of the synoptic-scale eddies modulated by the blocking flow ([Sisson and Gyakum 2004](#); [Zhou et al. 2009](#)). In our statistical and composite analyses, the different roles of different types of NAO regimes in the outbreak of European cold weather events are emphasized, although other large-scale patterns such as the eastern Atlantic pattern (EA) are found to affect the weather and climate over Europe ([Moore and Renfrew 2012](#)). Moreover, to further understand whether the European cold winters in recent years are related to  $\text{NAO}^+$  to  $\text{ENAO}^-$  transition events, we will calculate the frequency of  $\text{NAO}^+$  to  $\text{ENAO}^-$  transition events during 1978–2012 and examine its contribution to the variation of temperature and precipitation anomalies in different subregions of Europe. We will also contrast the impact of  $\text{ENAO}^-$  events associated with the  $\text{NAO}^+$  to  $\text{ENAO}^-$  transitions on the temperature and precipitation anomalies with those of in situ  $\text{WNAO}^-$ , in situ  $\text{ENAO}^-$ , and  $\text{WNAO}^-$  events (these events will be defined below) associated with the  $\text{NAO}^+$  to  $\text{WNAO}^-$  transitions.

This paper is arranged as follows: the data and methodology are described in [section 2](#). An analysis of the NAO transition event that occurred in January–February 2012 is presented in [section 3](#). It is shown that the outbreak of the extreme cold weather event over Europe in January–February 2012 is closely related to the occurrence of a  $\text{NAO}^+$  to  $\text{ENAO}^-$  transition event. In [section 4](#), we show the findings of a statistical analysis of the frequency of  $\text{NAO}^+$  to  $\text{ENAO}^-$  and  $\text{NAO}^+$  to  $\text{WNAO}^-$  transition events to emphasize the role of frequent  $\text{NAO}^+$  to  $\text{ENAO}^-$  transition events in the extreme cold events in recent winters. A comparison to other types of NAO events is made in [section 5](#). The conclusions and discussion are summarized in [section 6](#).

## 2. Data and methodology

In the present paper, we use the National Centers for Environmental Prediction–National Center for Atmospheric Research (NCEP–NCAR) daily mean, multi-level,  $2.5^\circ \times 2.5^\circ$  grid reanalysis for 1978–2012. The daily NAO index is defined as the principal component (PC) of the first rotated empirical orthogonal function (EOF) of the daily 500-hPa geopotential height poleward of  $20^\circ\text{N}$ , referred to as the PC index hereafter, which is available from the National Oceanic and Atmospheric

Administration (NOAA)/Climate Prediction Center (CPC) (<http://www.cpc.ncep.noaa.gov>). Moreover, we use the daily temperature and precipitation data from the European Climate Assessment and Dataset project (E-OBS gridded dataset) with  $0.5^\circ \times 0.5^\circ$  horizontal grid spacing for 1978–2012 to examine the variability of the precipitation and temperature anomalies for this period. In the following sections, the daily temperature (precipitation) anomaly is defined as a deviation of the daily temperature (precipitation) from the mean value for each particular day of a winter [November–March (NDJFM)] during the 1978/79–2011/12 winters (hereafter 1978–2012).

To identify the NAO event that occurred during the 2011/12 winter, we use a modified NAO index (Li and Wang 2003). This index is defined as the difference of the normalized SLP zonally averaged from  $80^\circ\text{W}$  to  $30^\circ\text{E}$  (from the western North Atlantic to the European continent) between  $35^\circ$  and  $65^\circ\text{N}$  (Li and Wang 2003), and referred to as the Li and Wang (LW) index hereafter. The value of the LW index may reflect the presence or absence of European blocking events because the calculation region of this index includes the longitudes from  $30^\circ\text{W}$  to  $30^\circ\text{E}$  where Euro–Atlantic blocking events are most frequently prevalent (Shabbar et al. 2001). When a blocking event follows an  $\text{NAO}^+$  event and is situated in the Atlantic basin, an  $\text{NAO}^+$  to  $\text{NAO}^-$  transition event can be detected with the PC index (Luo et al. 2012a,b) because  $\text{NAO}^-$  events correspond to the presence of blocking events over the North Atlantic or Greenland (Woollings et al. 2008). However, when blocking events remain over the European continent, it is difficult to observe such an  $\text{NAO}^+$  to  $\text{NAO}^-$  transition event in the PC index. But, the  $\text{NAO}^+$  to European blocking (in this study, a European blocking event is referred to as an  $\text{ENAO}^-$  event) transition event can be seen in the LW index as that index can represent an eastward displacement of the  $\text{NAO}^-$  dipole. Thus, the LW index can better represent the transition from an  $\text{NAO}^+$  event to an eastern Atlantic–European blocking event than the PC index. It is for this reason that the LW index is used to represent  $\text{ENAO}^-$  events in the present investigation.

Here, an NAO event is defined to take place if the LW index is equal to or greater than one standard deviation for at least three consecutive days. The same definition is used for the PC index. In situ NAO events are defined to be events that are not preceded by opposite phase events even though the term “in situ” refers to location, not time. However, in this paper in situ is still used to represent individual events similar to the definition of Luo et al. (2012a). Moreover, each event within the  $\text{NAO}^+$  to  $\text{NAO}^-$  transition must satisfy the above definition of

an NAO event as well as their total duration for the transition from one regime to another does not exceed 45 days (Luo et al. 2012a).

We further define the  $\text{NAO}^-$  event by the longitudinal location of the positive center of the  $\text{NAO}^-$  pattern for the  $\text{NAO}^+$  to  $\text{NAO}^-$  transition event. That is, those  $\text{NAO}^-$  events whose positive anomaly centers are located to the east (west) of  $10^\circ\text{W}$  are defined as  $\text{ENAO}^-$  ( $\text{WNAO}^-$ ) events. In this case, the  $\text{NAO}^+$  to eastern Atlantic–European blocking transition event can be named as a  $\text{NAO}^+$  to  $\text{ENAO}^-$  transition event. Similarly, the in situ  $\text{NAO}^-$  or blocking event with positive anomaly center located to the east (west) of  $10^\circ\text{W}$  is defined as the in situ  $\text{ENAO}^-$  ( $\text{WNAO}^-$ ) event. For the positive phase, the same definition can be made according to the zonal position of the negative anomaly center of the NAO pattern.

### 3. A case study of the NAO transition event in January–February 2012

#### a. An $\text{NAO}^+$ to $\text{ENAO}^-$ transition event

We show the evolution of the 300-hPa geopotential height field for every two days for the period from 13 January to 16 February 2012 in Fig. 2a. A similar flow evolution is also found for the 500-hPa height field (not shown). It is evident that upstream of the European continent, there is strong zonal flow represented by a strong geopotential height gradient indicative of a jet during the period from 18 to 22 January, corresponding to a  $\text{NAO}^+$  pattern (Fig. 2a). This  $\text{NAO}^+$  pattern can also be identified by the presence of a low-over-high dipole corresponding to an anomalously cold-over-warm pattern along the midlatitude jet core over the region from the Atlantic basin to the European continent (most evident on 18 and 22 January 2012). Feldstein (2003) and Benedict et al. (2004) also noted that the composite  $\text{NAO}^+$  pattern has such a typical low-over-high dipole structure. Moreover, a blocking circulation is seen to appear in the region from  $45^\circ$  to  $90^\circ\text{E}$ , downstream of the  $\text{NAO}^+$  pattern, as shown in Fig. 2a from 18 to 22 January. This European block is weak during the period from 21 to 23 January, but reintensifies and retrogrades after 23 January. An interesting feature is that a smaller-scale ridge seems to merge with a broader upstream ridge to form a larger-scale ridge that resembles an omega block, and then a closed high-latitude anticyclone breaks off from the ridge. During the following days, this retrograde block gradually moves into the eastern North Atlantic (Fig. 2a from 25 January to 6 February). If such a blocking flow retrogrades sufficiently far that it enters the North Atlantic basin, it may become a negative NAO ( $\text{NAO}^-$ ) event (Luo et al. 2007; Woollings et al. 2008). However,

the main body of the blocking flow remains located over the European continent during the period from 29 January to 6 February. This block may be called an eastern Atlantic–European block, as a small part of the block is located over North Atlantic. Here, we consider the eastern Atlantic–European block to be an ENAO<sup>-</sup> event based on the previously discussed definition of the ENAO<sup>-</sup> pattern, although the spatial scale of the blocking ridge in the unfiltered field (Fig. 2a) is relatively small (the planetary-scale component of the blocking flow has a scale comparable to that of the NAO<sup>-</sup>, not shown). In this case, the flow evolution of an NAO<sup>+</sup> event into an eastern Atlantic–European blocking event can be thought of as an NAO<sup>+</sup> to ENAO<sup>-</sup> transition event.

In the present paper, we will focus our attention on the impact of the NAO<sup>+</sup> to ENAO<sup>-</sup> transition event on the variation of temperature and precipitation anomalies over Europe rather than its physical mechanism. To see if the LW index can better reflect the transition of an NAO<sup>+</sup> event toward an ENAO<sup>-</sup> event than the PC index, we show the time evolution of the daily PC index as well as the SLP and 500-hPa LW indices during the period from 13 January to 16 February 2012 in Fig. 2b.

It is seen from Fig. 2b that the PC index exhibits mostly positive values from 8 January to 16 February 2012. The PC index of the strong zonal flow has a value that exceeds one standard deviation for at least three consecutive days on 18, 19, 20, and 21 January 2012. Thus, the 4-day duration of the positive NAO index qualifies this strong zonal flow as an NAO<sup>+</sup> regime. Naturally, this flow can be considered an NAO<sup>+</sup> event. The PC index reaches its maximum value at 19 January and then decays to a neutral value until 5 February. Thus, it appears that during the period from 13 January to 16 February 2012 the NAO identified by the PC index corresponds only to an NAO<sup>+</sup> event. However, the SLP LW index exhibits an evolution from a positive (from 13 to 21 January) to negative value (from 22 January to 13 February) during the period from 13 January to 16 February. Such variation is also seen at the 500-hPa level (Fig. 2b). Thus, the LW index identifies an NAO<sup>+</sup> to ENAO<sup>-</sup> transition event. In this transition event, the ENAO<sup>-</sup> event is evidently more persistent than the NAO<sup>+</sup> event, as indicated in Fig. 2b. Thus, this LW index is preferable for identifying the eastward-displaced NAO<sup>-</sup> event than is the PC index. Although the value of the LW index during the period from 8 January to 21 January is different from that of the PC index, the two types of indices exhibit a similar trend variation (solid and dashed lines in Fig. 2b). Thus, it is seen from a comparison with Fig. 1 that the phase of the NAO event cannot reflect the variation of the SAT over Europe during the 2011/12 winter (Fig. 1b).

Perhaps, the temporal change in the daily NAO index (Fig. 2b, solid and dashed) is more likely to be able to reflect the variation of the domain-averaged SAT over Europe (Fig. 2b, red). In section 3b, we will demonstrate from case and composite analyses that when an NAO<sup>+</sup> to ENAO<sup>-</sup> transition event takes place, the SAT and precipitation due to the transition from the NAO<sup>+</sup> to ENAO<sup>-</sup> patterns are more influenced than those due to other types of NAO<sup>-</sup> events such as in situ ENAO<sup>-</sup> and WNAO<sup>-</sup> events, as well as WNAO<sup>-</sup> events associated with the NAO<sup>+</sup> to WNAO<sup>-</sup> transition, as defined above.

### *b. Surface air temperature and precipitation anomalies associated with the NAO<sup>+</sup> to ENAO<sup>-</sup> transition event*

In the case study presented here, the time interval of the positive (negative) LW index, denoted by blue lines in Fig. 2b, is defined as an NAO<sup>+</sup> (ENAO<sup>-</sup>) period. The composite SAT and precipitation anomalies during the NAO<sup>+</sup> and ENAO<sup>-</sup> period for the NAO<sup>+</sup> to ENAO<sup>-</sup> transition event in Fig. 2b are shown in Fig. 3.

It is clear that during the NAO<sup>+</sup> period the positive SAT anomaly is mainly located over central and northern Europe (Fig. 3a). However, during the ENAO<sup>-</sup> period a negative SAT anomaly covers all of the European continent from 30°–75°N to 0°–60°E (Fig. 3b). Correspondingly, during the NAO<sup>+</sup> period, a positive precipitation anomaly is located over central Europe, and small regions of positive precipitation anomalies are located over northern and southern Europe (Fig. 3c). However, during the ENAO<sup>-</sup> period, positive precipitation anomalies are confined to southeastern Europe along with a small positive precipitation anomaly over central Europe (Fig. 3d). Because the SAT anomaly changes from a positive anomaly over central and northern Europe to a persistent negative anomaly over all of the European continent, it is concluded that the extreme cold event over Europe in January–February 2012 is closely tied to the large-scale regime transition from an NAO<sup>+</sup> event to a long-lasting ENAO<sup>-</sup> event.

To further examine the effect of the NAO transition event on the SAT and precipitation anomalies over different latitudinal regions of the European continent (10°W–60°E), we divide Europe into three subregions: northern (60°–75°N), central (45°–60°N), and southern (30°–45°N) Europe, as described in Fig. 3b where the horizontal lines separate the three domains.

The temporal variation of the SAT and precipitation anomalies averaged over three different subregions for an NAO<sup>+</sup> to ENAO<sup>-</sup> transition event from 13 January to 15 February 2012 in Fig. 2a are shown in Fig. 4. It is seen in Fig. 4a that during the period from 23 January to

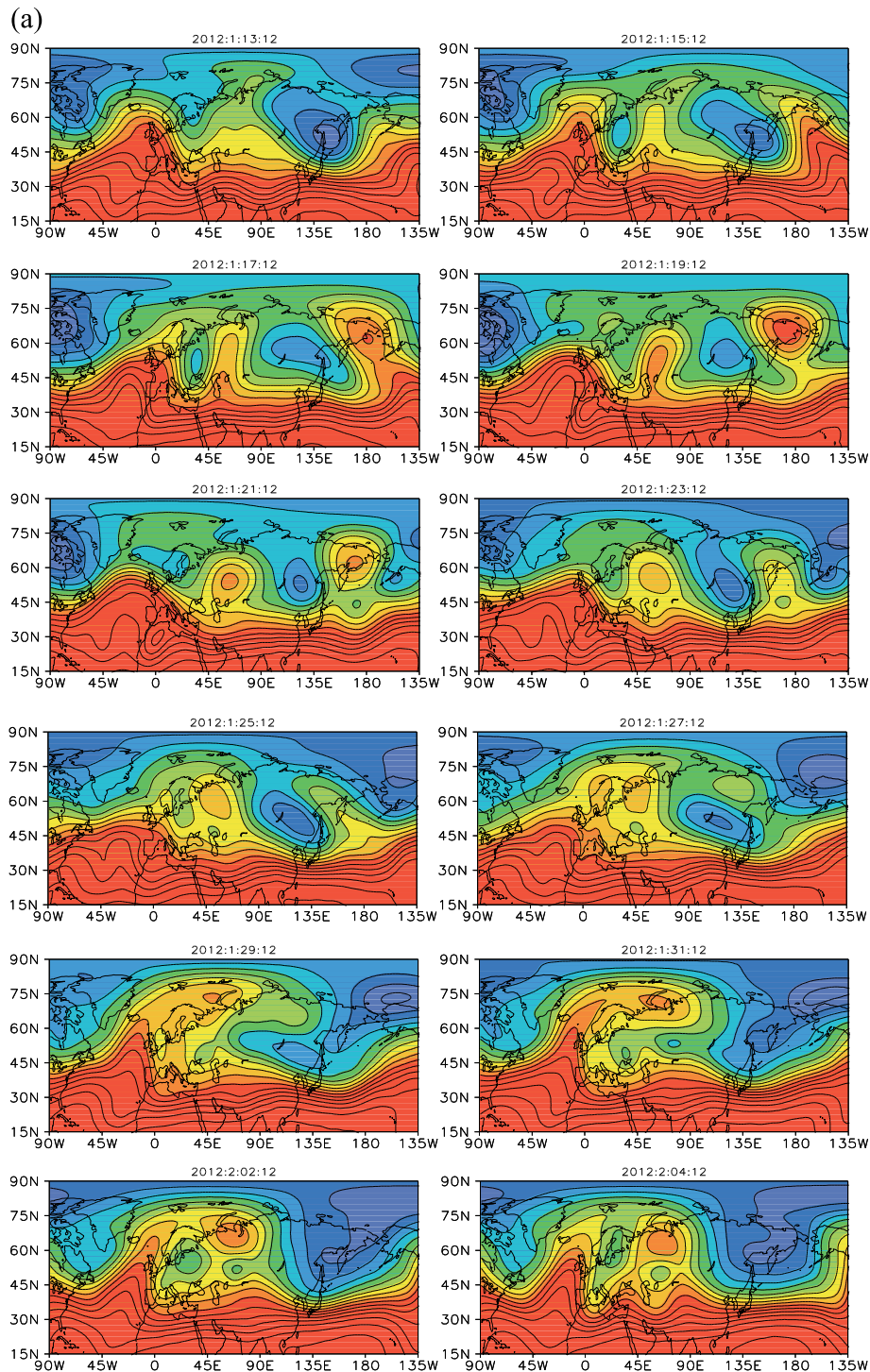


FIG. 2. (a) Time sequences of 300-hPa geopotential height (gpm) at 2-day intervals from an NAO<sup>+</sup> event (19 to 23 Jan) to an ENAO<sup>-</sup> event (27 Jan to 14 Feb) during the period from 13 Jan to 16 Feb 2012 and (b) its corresponding normalized daily NAO indices according to the definitions of the PC and LW indices. A five-point space (time) smoothing is applied to the height fields (time series). The blue line in (b) denotes the time interval for composites of temperature and precipitation. The shading in (a) is according to the color bar in gpm, where red (blue) denotes high (low) geopotential height and contours are drawn from 8200 to 9700 gpm with a 100-gpm interval. In (b) the PC index is marked with the dotted line, and the SLP (500 hPa) LW index is the solid line without (with) dots. The time series of the normalized SAT anomaly averaged over European continent (30°–75°N, 10°W–60°E) is shown in (b) (red). The NAO<sup>+</sup> and ENAO<sup>-</sup> epochs of the NAO<sup>+</sup> to ENAO<sup>-</sup> transition event are indicated in (b) (blue).

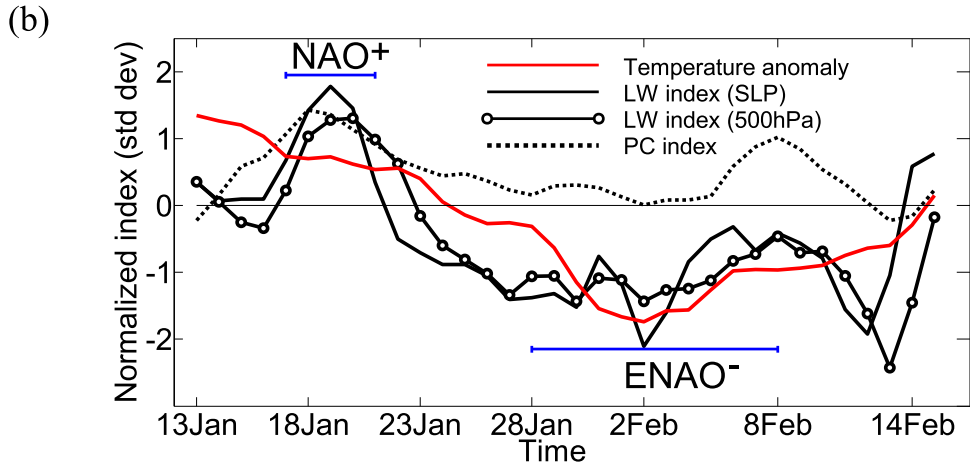
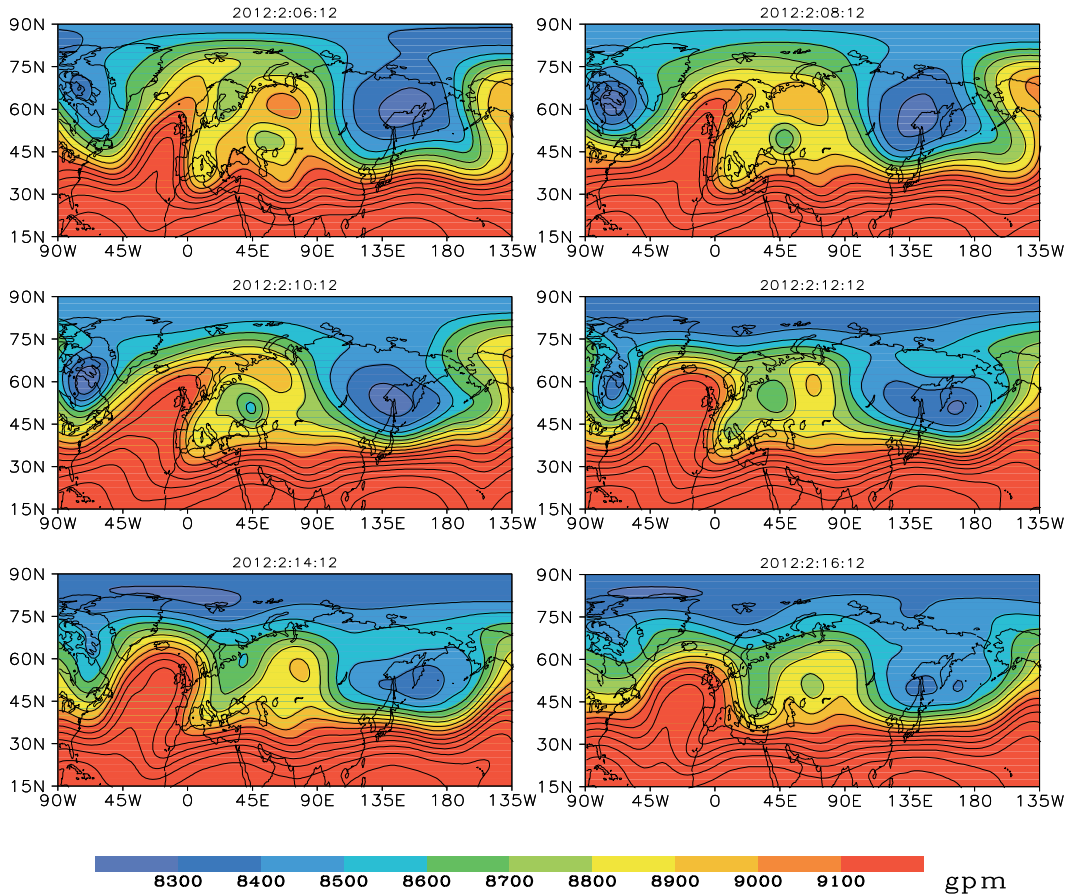


FIG. 2. (Continued)

15 February the regional average SAT anomalies in all three European subregions show a marked decline after the LW index begins to decline during the NAO<sup>+</sup> to ENAO<sup>-</sup> transition, and the SAT increase seems to occur with the LW index increase. The SAT anomalies from 13 January to 15 February in northern, central, and

southern Europe (Fig. 4a) exhibit positive correlations of 0.81, 0.84, and 0.66, respectively. The values are statistically significant at the 95% confidence level (Glahn 1968). Over northern and central Europe, the SAT anomaly and the LW index exhibit almost an in-phase correlation, but over southern Europe the SAT anomaly

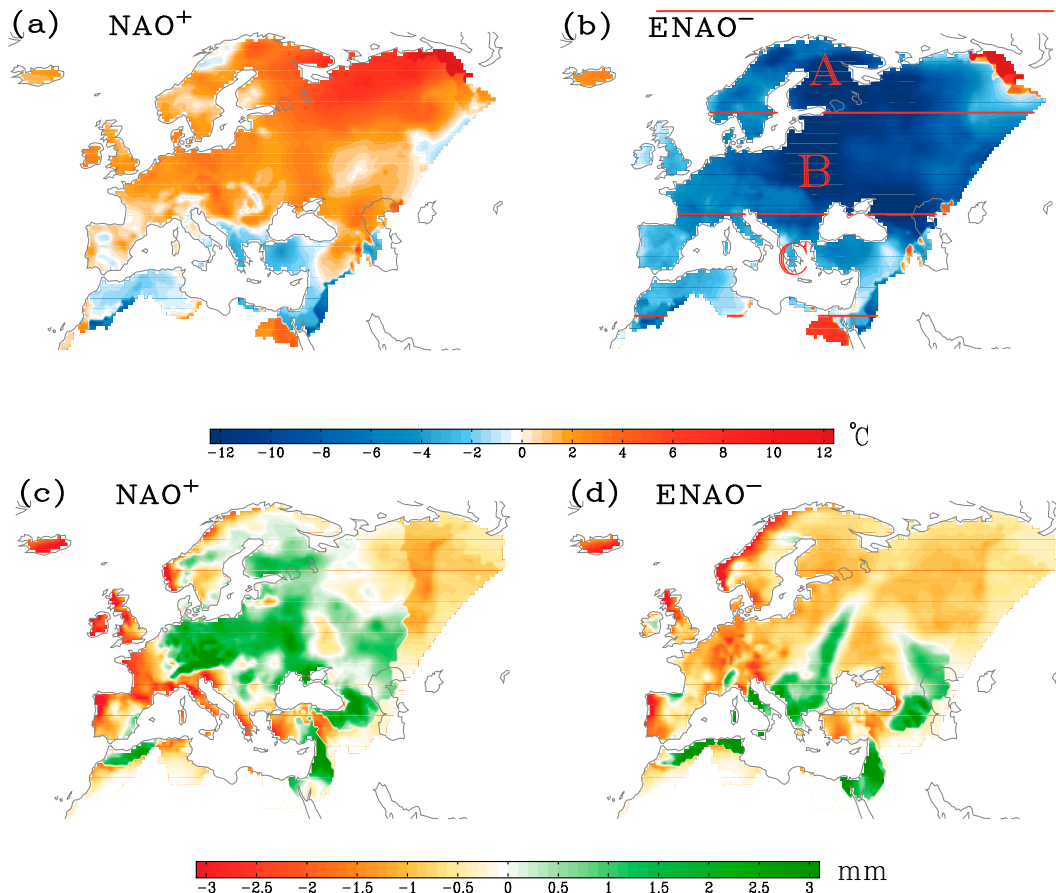


FIG. 3. Composites of (a),(b) SAT anomalies and (c),(d) precipitation anomalies during the (a),(c)  $\text{NAO}^+$  (5 days around the peak at 19 Jan) and (b),(d)  $\text{ENAO}^-$  (10 days around the peak at 2 Feb) periods of the  $\text{NAO}^+$  and  $\text{ENAO}^-$  transition event from 13 Jan to 14 Feb 2012 as shown in Fig. 2b. In (b), the A, B, and C represent northern ( $60^\circ\text{--}75^\circ\text{N}$ ), central ( $45^\circ\text{--}60^\circ\text{N}$ ), and southern ( $30^\circ\text{--}45^\circ\text{N}$ ) Europe, respectively.

exhibits a delayed correlation with the LW index, whose correlation coefficient is 0.86 (0.92) at lag 3 (5) days. These correlations reflect that a negative SAT anomaly forms over northern and central Europe, and then extends toward southern Europe during the  $\text{NAO}^+$  to  $\text{ENAO}^-$  transition.

We also find that the domain-averaged precipitation anomaly and the LW index exhibit positive correlations of 0.25 and 0.83 over northern and central Europe, respectively, but a negative correlation of  $-0.48$  over southern Europe (Fig. 4b). These correlations are statistically significant at the 95% confidence level only over central and southern Europe. Thus, it is easy to see that when the LW index changes from a positive to a negative value, a positive precipitation anomaly can be seen over southern Europe (from 21 January to 7 February). This indicates that there is a marked increase in the precipitation over southern Europe as the  $\text{NAO}^+$  event transitions into an  $\text{ENAO}^-$  event. Over northern Europe and most parts of central Europe the precipitation anomalies

are negative as the LW index becomes negative. The reason that we cannot observe a positive precipitation anomaly over northern Europe when the LW index is negative is because precipitation mainly occurs over the Norwegian and Barents Seas and along the northernmost coast of northern Europe. On the other hand, there is a marked decrease in the SAT as well as an increase in precipitation over southern Europe during the  $\text{ENAO}^-$  period and the extreme low temperatures cover almost all of Europe during the  $\text{ENAO}^-$  period (Fig. 4b). Therefore, it is thought that the regime transition from a  $\text{NAO}^+$  to a long-lasting  $\text{ENAO}^-$  event may play a crucial role in the outbreak of the intense extreme cold event over Europe in January–February 2012.

### c. Role of the storm track associated with the $\text{NAO}^+$ to $\text{ENAO}^-$ transition event on the extreme cold weather

It has been recognized that the position of synoptic-scale transient eddies in a storm track can in part

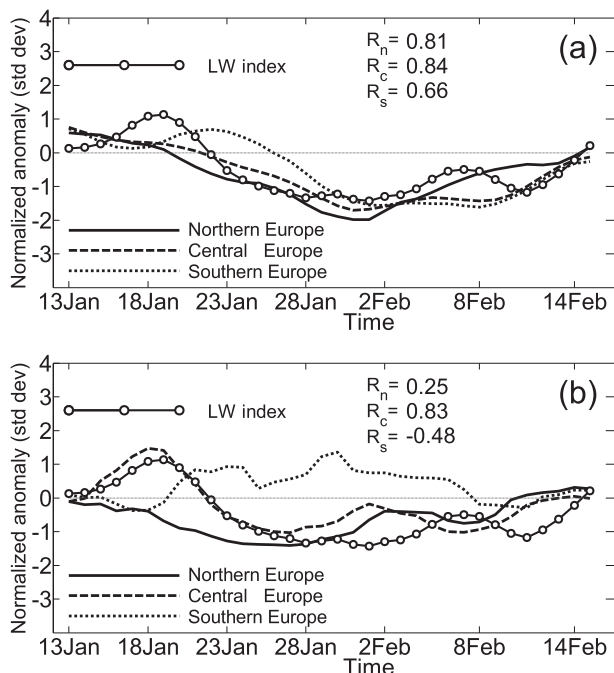


FIG. 4. Time series of (a) daily regional average SAT anomalies and (b) precipitation anomalies in the three European subregions from 8 Jan to 21 Feb 2012. The LW index is indicated by the solid line with dots. A five-point smoothing is used for all the time series. The correlation coefficients  $R_n$  (northern Europe),  $R_c$  (central Europe), and  $R_s$  (southern Europe) between the LW index and the time series of the regional average SAT anomalies during the period from 8 Jan to 19 Feb are also indicated.

determine the spatial distribution of the temperature and precipitation anomalies (Sisson and Gyakum 2004; Zhou et al. 2009; Archambault et al. 2010). The blocking anticyclone over Europe (ENAO<sup>-</sup> event) affects the temperature and precipitation in the blocking region and its adjacent regions by modulating the path of synoptic-scale eddies (e.g., Pfahl and Wernli 2012). Thus, it is important to examine the relationship between the synoptic-scale eddy activity, temperature, and precipitation associated with the NAO<sup>+</sup> to ENAO<sup>-</sup> transition event.

Here, the 2.5–7-day, synoptic-scale, eddy kinetic energy (EKE) at 300 hPa is obtained by applying the Butterworth filter (Hamming 1989). To see the variation of the EKE, we define the daily EKE anomaly as the deviation of the daily EKE from the winter mean EKE during 1978–2012. The composite 300-hPa EKE anomalies during the NAO<sup>+</sup> and ENAO<sup>-</sup> periods for the NAO<sup>+</sup> to ENAO<sup>-</sup> transition event are shown in Figs. 5a,b. Correspondingly, the time series of the normalized domain-averaged EKE anomalies in the three subregions of the European continent are shown in Fig. 5c. We see in Figs. 5a,b that during the NAO<sup>+</sup> period, the composite

EKE anomaly over the North Atlantic shows a single-branched structure (Fig. 5a), whose maximum core (hereafter storm track) is oriented along the west–east direction. However, during the ENAO<sup>-</sup> period, the composite EKE anomaly is split into two branches and exhibits a double storm track structure: one storm track located over the Norwegian and Barents Seas and the other storm track exhibiting a northwest–southeast orientation over southern Europe (Fig. 5b). Thus, the splitting of the Atlantic storm track over the European continent likely plays an important role in determining the spatial distribution of the precipitation anomalies observed during the ENAO<sup>-</sup> period (Fig. 3d). Results from the nonlinear multiscale interaction models of blocking and NAO events demonstrate that during blocking or NAO<sup>-</sup> episodes the Atlantic storm track often splits into two branches as a result of the feedback of the blocking or NAO<sup>-</sup> anomaly (Luo 2005), but maintains a single branch during the NAO<sup>+</sup> period (Luo et al. 2007). Thus, the Atlantic storm track can evolve from a single branch into two branches around the blocking or ENAO<sup>-</sup> region as the NAO<sup>+</sup> event transitions into an ENAO<sup>-</sup> event. Since the storm track and NAO<sup>-</sup> or blocking pattern in a planetary-scale field exhibit a symbiotic relation during their interaction as noted by many investigators (Cai and Mak 1990; Luo 2005; Luo et al. 2007), the double storm tracks shown in Fig. 5b may be persistent because of the long-lived eastern Atlantic–European blocking or ENAO<sup>-</sup> pattern.

It is found that the normalized EKE anomaly time series and LW index exhibit a negative correlation of  $-0.58$  ( $-0.43$ ) over northern (southern) Europe, but a positive correlation of  $0.23$  over central Europe (Fig. 5c). This shows that when the LW index varies from a positive to a negative value due to the NAO<sup>+</sup> to ENAO<sup>-</sup> transition, the EKE is enhanced over southern and northern Europe (including some parts of the Norwegian and Barents Seas). The only correlations that are found to be statistically significant at the 95% confidence level are those over southern and northern Europe. However, the same correlations computed for the LW index leading the EKE index by 1 day yield values of  $-0.59$ ,  $0.4$ , and  $-0.34$  for  $R_n$ ,  $R_c$ , and  $R_s$ , respectively, values that are statistically significant at the 95% confidence level. The correlations are still significant over northern and central Europe, but not significant over southern Europe when the LW index leads the EKE index by 2 days. Thus, the variation of the storm track over Europe is likely to be related to the NAO<sup>+</sup> to ENAO<sup>-</sup> transition.

To further understand the relationship between the variation of the EKE anomaly and the SAT and

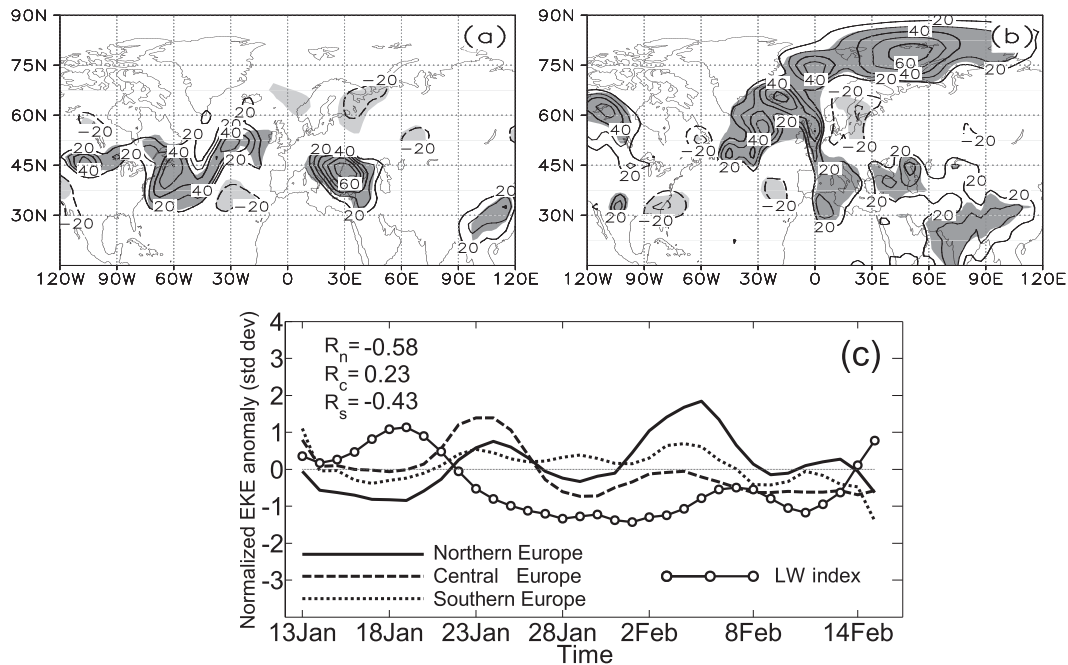


FIG. 5. Composites of anomalous synoptic-scale eddy kinetic energy (EKE) ( $\text{m}^2 \text{s}^{-2}$ ) during the (a)  $\text{NAO}^+$  (5 days around the peak at 19 Jan) and (b)  $\text{ENAO}^-$  (10 days around the peak at 2 Feb) periods of the  $\text{NAO}^+$  and  $\text{ENAO}^-$  transition event as shown in Fig. 2, and (c) the time series of the daily EKE anomaly during the period from 8 Jan to 21 Feb 2012 for three different subregions of Europe. A five-point smoothing is used for all the time series. The correlation coefficients  $R_n$ ,  $R_c$ , and  $R_s$  between the LW index and the regional average EKE time series in the three subregions for the period from 8 Jan to 19 Feb are also indicated. In (a) and (b), the dark (light gray) shading represents positive (negative) EKE anomaly region that exceeds the 99% confidence level for a two-sided Student's  $t$  test.

precipitation anomalies, we calculate the correlation between the normalized EKE time series and the change of the domain-averaged SAT and precipitation anomalies (not shown). It is found that the EKE time series exhibits a negative correlation of  $-0.54$  ( $-0.01$ ) with the domain-averaged SAT anomaly time series over northern (southern) Europe, and a positive correlation of  $0.47$  over central Europe. The correlation coefficient between the EKE and SAT anomalies over southern Europe is  $-0.51$  when the EKE anomaly leads the SAT anomaly by 3 days. Thus, the negative SAT anomaly increases over northern and southern Europe are related to the EKE anomaly increases over the same regions, while the SAT declines over central Europe when the EKE anomaly decreases (Fig. 5c). We see that the EKE time series exhibits negative and positive correlations of  $-0.05$  and  $0.67$  with the domain-averaged precipitation anomaly time series over northern and southern Europe, respectively, and a weak positive correlation of  $0.12$  over central Europe. Of the three precipitation correlations, the value for southern Europe is the only one that is statistically significant. This suggests that when the EKE is enhanced over northern and southern Europe due to the transition of the  $\text{NAO}^+$

event toward the  $\text{ENAO}^-$  event, the precipitation anomalies tend to be above normal over southern Europe. Thus, the SAT and precipitation changes over Europe in January–February 2012 may be linked to the  $\text{NAO}^+$  to  $\text{ENAO}^-$  transition event via changes in the associated storm track.

Recently, Archambault et al. (2010) found that cool-season (November–April) northeastern U.S. (NE) precipitation tends to be enhanced (suppressed) during the  $\text{NAO}^+$  to  $\text{NAO}^-$  ( $\text{NAO}^-$  to  $\text{NAO}^+$ ) transition. They further noted that the variation of the NE precipitation is closely related to the NAO transition events rather than individual NAO events. In the present study we have found for the  $\text{NAO}^+$  to  $\text{ENAO}^-$  transition events that the SAT and precipitation anomaly patterns over Europe are distinctly different before and after the transition, but their anomaly changes are relatively weak near the transition point within the  $\text{NAO}^+$  to  $\text{ENAO}^-$  transition event (Fig. 4). Thus, the regime transition from the  $\text{NAO}^+$  regime to an  $\text{ENAO}^-$  regime can induce drastic changes in the winter SAT and precipitation over Europe. This is because the cold air outbreak takes place subsequently when an  $\text{ENAO}^-$  event occurs.

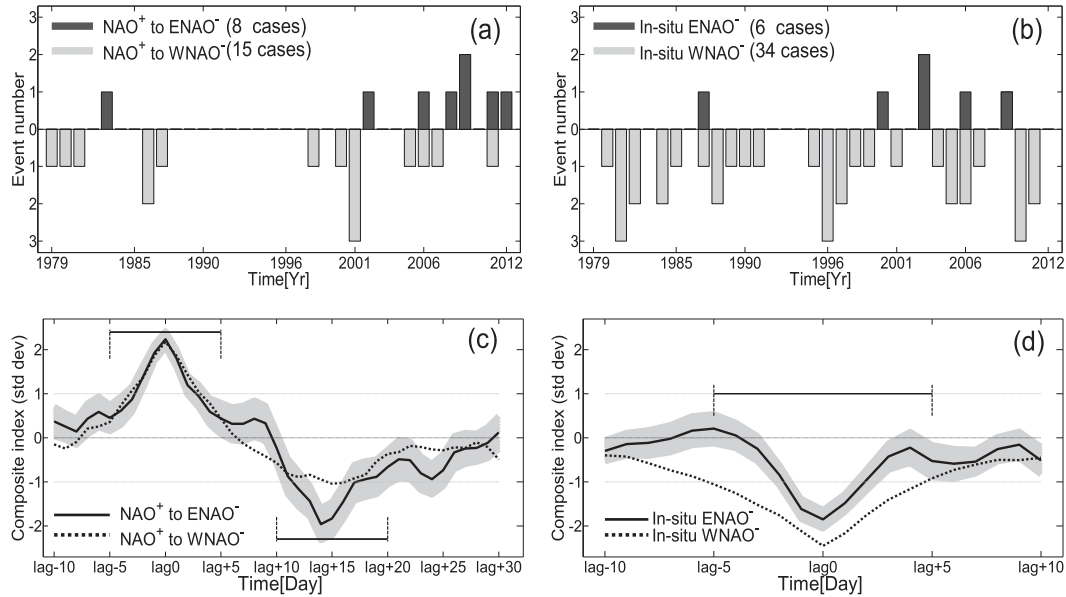


FIG. 6. Time series of the number of  $\text{NAO}^-$  events for the (a)  $\text{NAO}^+$  to  $\text{NAO}^-$  transition events and for the (b) in situ  $\text{NAO}^-$  events based on the LW index. In (a) 1979 represents 1978/79 and in (b) 2012 represents 2011/12 and the black (gray) shading denotes the number of  $\text{ENAO}^-$  ( $\text{WNAO}^-$ ) events, respectively. Composites of the daily LW NAO index for the  $\text{NAO}^+$  transition and in situ events are shown in (c) and (d), respectively, where lag 0 day denotes the day with the strongest NAO amplitude. The brackets in (c) and (d) denote the time interval used for composites of temperature and precipitation. The gray shading in (c) denotes the 95% confidence limit for a Monte Carlo test. The line outside the shading area is statistically significant.

#### 4. Composite of $\text{NAO}^+$ to $\text{NAO}^-$ transition events and its relationship to temperature and precipitation variations

The aim of this section is to examine whether the European extreme cold events observed in recent winters are related to  $\text{NAO}^+$  to  $\text{ENAO}^-$  transition events. To illustrate the difference between the  $\text{NAO}^+$  transition and in situ  $\text{NAO}$  events, we show in Figs. 6a,b the time variations of the frequencies of the  $\text{NAO}^+$  to  $\text{ENAO}^-$  and  $\text{NAO}^+$  to  $\text{WNAO}^-$  transition events and the  $\text{ENAO}^-$  and  $\text{WNAO}^-$  in situ events during 1978–2012. Here, the winter is defined to extend from November to March. It is seen that during 1978–2012 the frequency of in situ  $\text{NAO}^-$  events is much higher than that of  $\text{NAO}^+$  to  $\text{NAO}^-$  transition events, but the  $\text{NAO}^+$  to  $\text{NAO}^-$  transition events become relatively more frequent after 1995. In particular, during 2005–12 the  $\text{NAO}^+$  to  $\text{ENAO}^-$  transition events is more frequent than  $\text{NAO}^+$  to  $\text{WNAO}^-$  transition events (Fig. 6a). We also find that the number of in situ  $\text{ENAO}^-$  events is much less than that of in situ  $\text{WNAO}^-$  events during 1978–2012, and also lower than that of the  $\text{NAO}^+$  to  $\text{ENAO}^-$  transition events especially during 2005–12 (Fig. 6b). Thus, it is possible that the frequent occurrence of the intraseasonal  $\text{NAO}^+$  to  $\text{ENAO}^-$  transition events makes an important

contribution to the extreme cold weather events over the European continent in recent winters.

The composite LW NAO indices of the  $\text{NAO}^+$  to  $\text{ENAO}^-$  (solid) and  $\text{NAO}^+$  to  $\text{WNAO}^-$  (dashed) transition events are shown in Fig. 6c, while Fig. 6d corresponds to those of in situ  $\text{ENAO}^-$  and  $\text{WNAO}^-$  events. It is noted that the amplitude of the composite NAO index when it is negative is stronger for the  $\text{NAO}^+$  to  $\text{ENAO}^-$  transition events than for the  $\text{NAO}^+$  to  $\text{WNAO}^-$  transition events (Fig. 6c), while it is weaker for the in situ  $\text{ENAO}^-$  events than it is for the in situ  $\text{WNAO}^-$  events (Fig. 6d).

We will examine the difference between the temperature and precipitation anomalies for the  $\text{NAO}^+$  to  $\text{ENAO}^-$  and  $\text{NAO}^+$  to  $\text{WNAO}^-$  transition events as well as the difference between the in situ  $\text{ENAO}^-$  and  $\text{WNAO}^-$  events. We show the composite SAT patterns for the  $\text{NAO}^+$  and  $\text{ENAO}^-$  regimes associated with the  $\text{NAO}^+$  to  $\text{ENAO}^-$  transition events and their difference in Fig. 7, while the composite SAT anomaly patterns for the  $\text{NAO}^+$  and  $\text{WNAO}^-$  regimes of the  $\text{NAO}^+$  to  $\text{WNAO}^-$  transition events and their difference are shown in Fig. 8. Note that for the  $\text{NAO}^+$  to  $\text{NAO}^-$  transition events the time interval for the composite of  $\text{NAO}^+$  events is from lag  $-5$  to lag  $+5$  days (hereafter the “ $\text{NAO}^+$  period”), while the time interval for the composite of  $\text{ENAO}^-$  ( $\text{WNAO}^-$ ) events is from lag

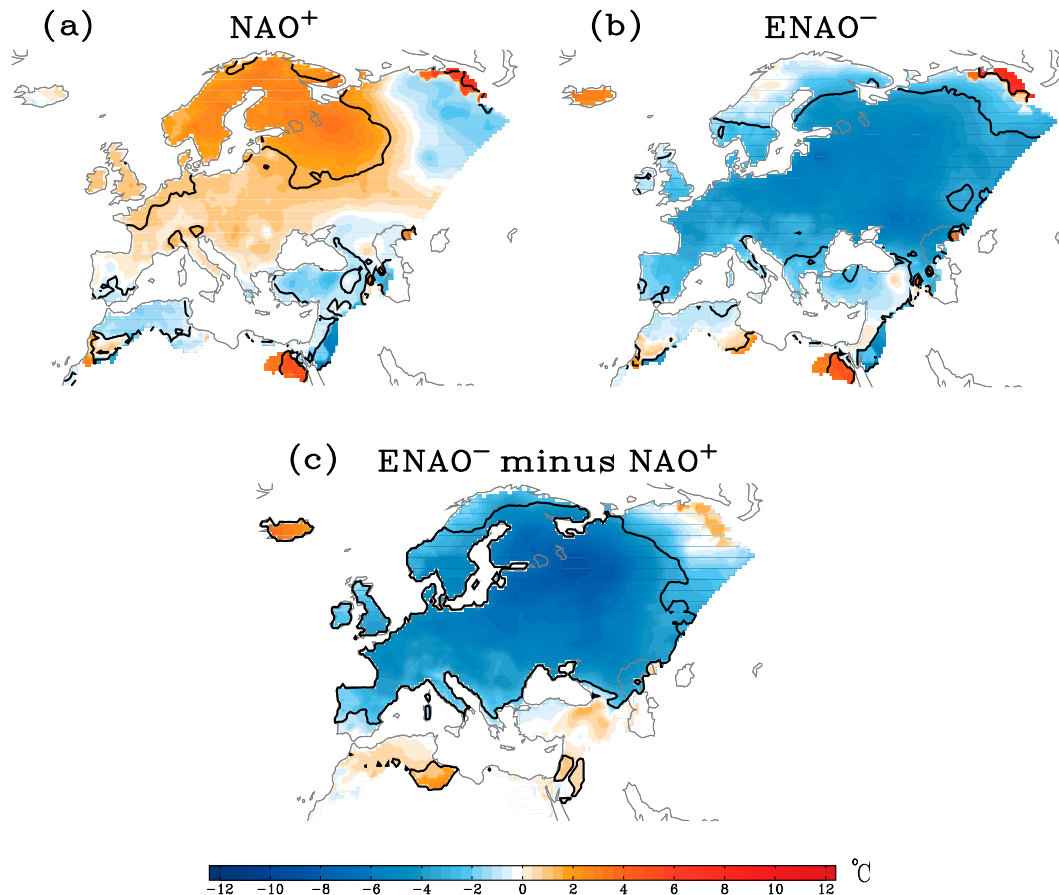


FIG. 7. Composites of SAT anomalies for the (a)  $\text{NAO}^+$  and (b)  $\text{ENAO}^-$  events of the  $\text{NAO}^+$  to  $\text{ENAO}^-$  transition events (eight cases) and (c) their difference. The composite of  $\text{NAO}^+$  events is performed from lag  $-5$  to lag  $+5$  days, where lag 0 day denotes the day with the largest amplitude, while the composite of  $\text{ENAO}^-$  events is performed from lag  $+10$  to lag  $+20$  days. Solid lines denote the regions that exceeded the 99% confidence level for a two-sided Student's  $t$  test.

$+10$  to lag  $+20$  days [hereafter the “ $\text{ENAO}^-$  ( $\text{WNAO}^-$ ) period”]. For in situ NAO events, the time interval of the composite is from lag  $-5$  to lag  $+5$  days. For the  $\text{NAO}^+$  to  $\text{ENAO}^-$  transition event there is a strong positive SAT anomaly over northern Europe and a small part of central Europe during the  $\text{NAO}^+$  period (Fig. 7a), and a strong negative SAT anomaly over the majority of Europe during the  $\text{ENAO}^-$  period (Fig. 7b). The regions are significant at the 95% confidence level for a two-sided Student's  $t$  test (Livezey and Chen 1983). Thus, a marked decrease in the SAT is seen over all of Europe as the  $\text{NAO}^+$  event transitions into an  $\text{ENAO}^-$  event. This can be seen from the difference of the composite SAT anomaly between both phases of the  $\text{NAO}^+$  to  $\text{ENAO}^-$  transition event (Fig. 7c). Our calculation further demonstrates that for six (1983, 2006, 2008, 2009, 2011, and 2012) out of eight  $\text{NAO}^+$  to  $\text{ENAO}^-$  transition events, as shown in Fig. 6a, the composite SAT anomaly during the  $\text{ENAO}^-$  period

(from lag 10 to lag 20 days, where lag 15 day denotes the day with the strongest amplitude of the  $\text{ENAO}^-$  anomaly for each  $\text{ENAO}^-$  event) looks similar to that in Fig. 7b (not shown). As a result, the SAT anomaly pattern in January–February 2012 is characteristic of the  $\text{NAO}^+$  to  $\text{ENAO}^-$  transition events in other winters. This can substantiate our claim that the extreme cold event over Europe in January–February 2012 is not an exceptional case.

For the  $\text{NAO}^+$  to  $\text{WNAO}^-$  transition events, the composite SAT pattern shows strong positive anomalies over central Europe and a small part of northern Europe during the  $\text{NAO}^+$  period (Fig. 8a), while the strong negative anomalies are located over northern Europe and western Europe during the  $\text{WNAO}^-$  period (Fig. 8b). We also see from the difference of the composite SAT anomaly between the  $\text{NAO}^+$  and  $\text{WNAO}^-$  periods that the decline of the SAT is much smaller and occurs over a smaller area (Fig. 8c) than during the

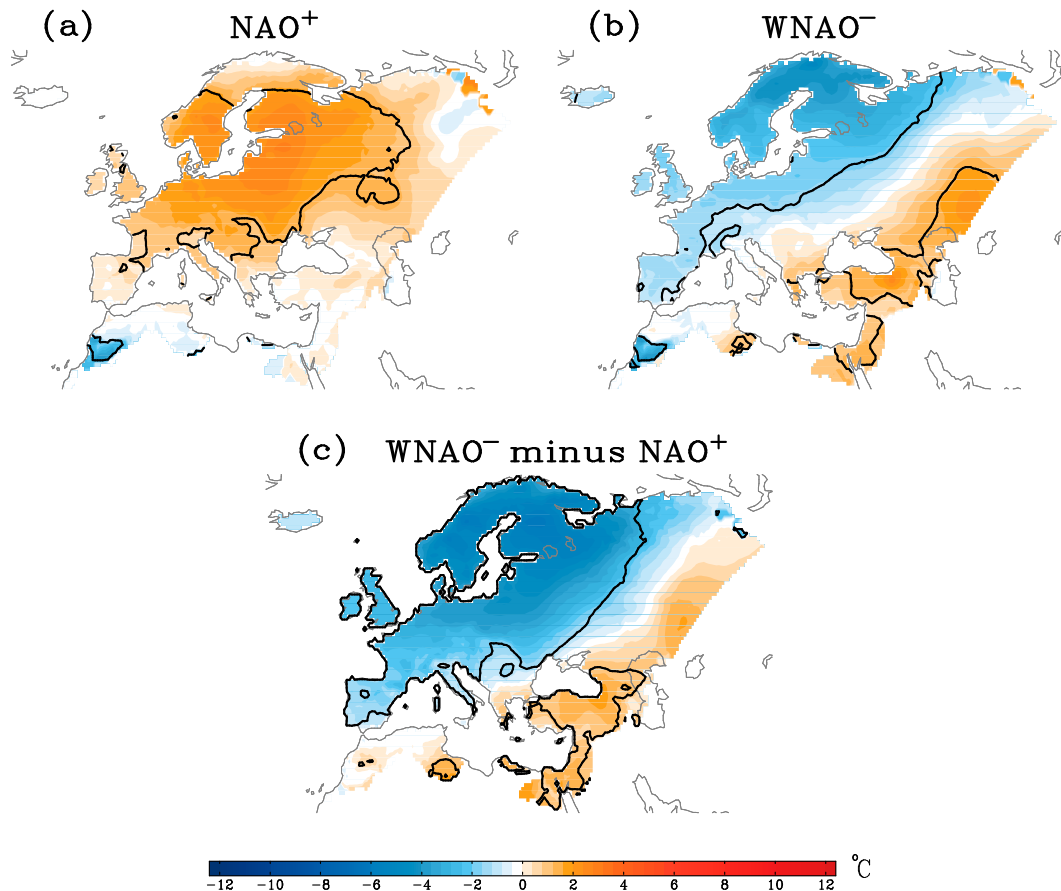


FIG. 8. As in Fig. 7, but for  $\text{NAO}^+$  to  $\text{WNAO}^-$  transition events (15 cases).

$\text{NAO}^+$  to  $\text{ENAO}^-$  transition events (Fig. 7c). A comparison between Figs. 7c and 8c further shows that the amplitude of the SAT decline is larger for the  $\text{NAO}^+$  to  $\text{ENAO}^-$  transition events than for  $\text{NAO}^+$  to  $\text{WNAO}^-$  transition events. Thus, the negative SAT anomaly over Europe occurs over a more widespread region and is more intense for the  $\text{ENAO}^-$  pattern than for the  $\text{WNAO}^-$  pattern. The corresponding composite precipitation anomaly patterns of these events are shown in Figs. 9 and 10, respectively. It is seen for the  $\text{NAO}^+$  to  $\text{ENAO}^-$  transition events that large precipitation anomalies are situated over central Europe and a small fraction of southern Europe for the  $\text{NAO}^+$  regime (Fig. 9a), but over southern Europe for the  $\text{ENAO}^-$  regime. The difference of the composite precipitation pattern over Europe between two phases of the NAO transition events is also significant at the 95% confidence level for a two-sided Student's  $t$  test (Fig. 9c). For the  $\text{NAO}^+$  to  $\text{WNAO}^-$  transition events, a large amount of precipitation is found over northern Europe and a small fraction of central Europe during the  $\text{NAO}^+$  period (before the transition) (Fig. 10a), and over

southern Europe and the eastern part of central Europe during the  $\text{WNAO}^-$  period (after the transition) (Fig. 10b). It is also easily seen from a comparison of Fig. 10c with Fig. 9c that the variation of the composite precipitation anomaly for the transition from the  $\text{NAO}^+$  to  $\text{WNAO}^-$  regime is distinctly different from that for the transition from the  $\text{NAO}^+$  to  $\text{ENAO}^-$  regime.

We show in Fig. 11 the SAT and precipitation time series over Europe and its three subregions for the  $\text{NAO}^+$  to  $\text{ENAO}^-$  transition events, where the correlation coefficients with the LW index are indicated. Correspondingly, for the  $\text{NAO}^+$  to  $\text{WNAO}^-$  transition events the SAT and precipitation time series over all of Europe and its three subregions are shown in Fig. 12. It is seen from a comparison between Figs. 11a and 12a that the decline of the SAT anomaly seems to be more pronounced over Europe for the  $\text{ENAO}^-$  pattern than for the  $\text{WNAO}^-$  pattern. A markedly persistent decline trend of the SAT is also seen over northern, central, and southern Europe for the  $\text{NAO}^+$  to  $\text{ENAO}^-$  transition events (Figs. 11c,d). This may be because the  $\text{ENAO}^-$  regime is more intense than the  $\text{WNAO}^-$  regime

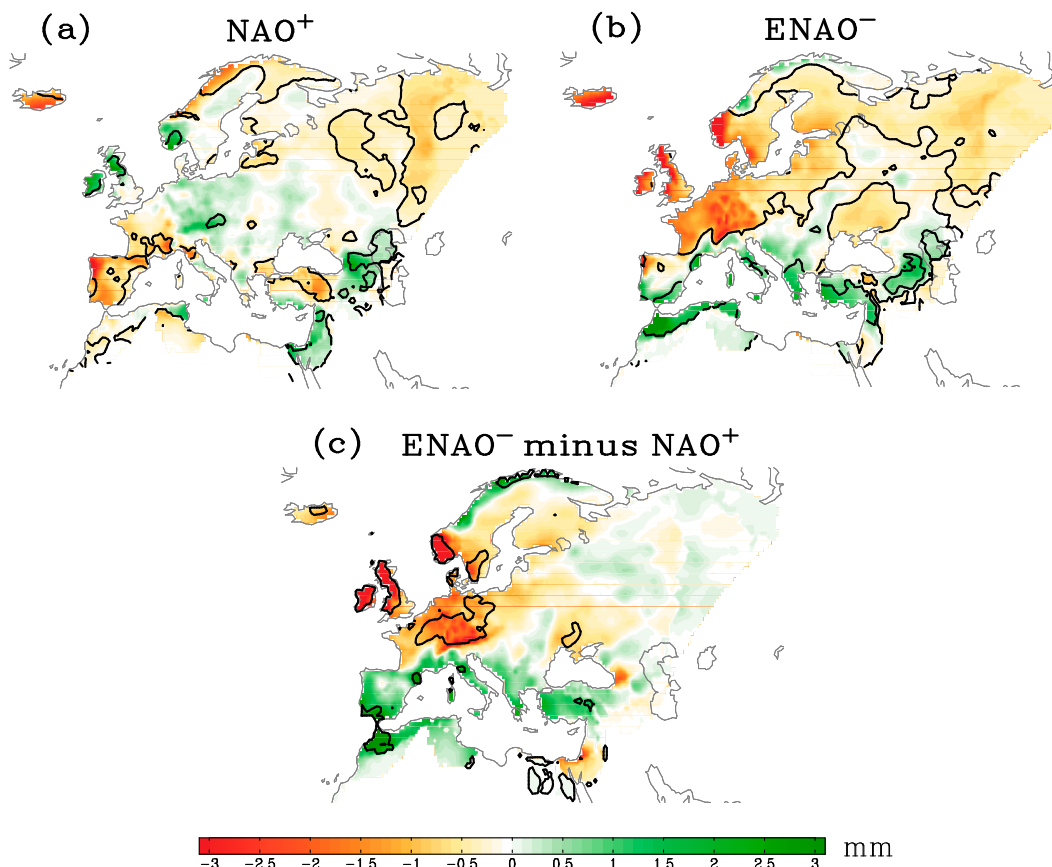


FIG. 9. Composites of precipitation anomalies for the (a)  $\text{NAO}^+$  and (b)  $\text{ENAO}^-$  events of the  $\text{NAO}^+$  to  $\text{ENAO}^-$  transition events (eight cases) and (c) their difference. The  $\text{NAO}^+$  composite is performed from lag  $-5$  to lag  $+5$  days, where lag 0 day denotes the day with the largest amplitude, while the  $\text{ENAO}^-$  composite is performed from lag  $+10$  to lag  $+20$  days. Solid lines denote the regions of anomalies that exceeded the 99% confidence level for a two-sided Student's  $t$  test.

(Fig. 6c). A further comparison indicates that the precipitation is enhanced over southern (central and southern) Europe as the  $\text{NAO}^+$  regime evolves into an  $\text{ENAO}^-$  ( $\text{WNAO}^-$ ) regime. The calculation shows that there is a positive correlation of 0.88 (0.83) between the LW index and SAT anomaly over Europe for the  $\text{NAO}^+$  to  $\text{ENAO}^-$  ( $\text{NAO}^+$  to  $\text{WNAO}^-$ ) transition events (Figs. 11a and 12a). Moreover, the correlation coefficient of the SAT anomaly with the LW index is 0.52, 0.91, and 0.59 over northern, central, and southern Europe, respectively, for the  $\text{NAO}^+$  to  $\text{ENAO}^-$  transition event, while it is 0.81, 0.79, and  $-0.35$  in the three subregions for the  $\text{NAO}^+$  to  $\text{WNAO}^-$  transition event. These correlations are all statistically significant at the 95% confidence level. The SAT anomaly over southern Europe exhibits a maximum correlation of 0.77 with the LW index at lag  $+3$  days for the  $\text{NAO}^+$  to  $\text{ENAO}^-$  transition event (Fig. 11d), and a maximum anticorrelation of  $-0.78$  with the LW index at lag 5 days for the  $\text{NAO}^+$  to  $\text{WNAO}^-$  transition event (Fig. 12d).

Thus, it is clear that a marked decline of the SAT can take place over all of the European continent for the  $\text{NAO}^+$  to  $\text{ENAO}^-$  transition event, but only over central and northern Europe for the  $\text{NAO}^+$  to  $\text{WNAO}^-$  transition event. This further indicates that a persistent marked decline of the SAT over southern Europe can be attributed to the  $\text{NAO}^+$  to  $\text{ENAO}^-$  transition events. As a result, the impact of the  $\text{NAO}^+$  to  $\text{ENAO}^-$  transition event on the decline of the SAT over Europe is more widespread than that of the  $\text{NAO}^+$  to  $\text{WNAO}^-$  transition event. This supports the results obtained from the case analyzed in section 2. The increase in the positive precipitation anomaly is relatively prominent in central and southern Europe for the  $\text{WNAO}^-$  regime of the  $\text{NAO}^+$  to  $\text{WNAO}^-$  transition event (Figs. 12b–d), but only in southern Europe for the  $\text{ENAO}^-$  regime of the  $\text{NAO}^+$  to  $\text{ENAO}^-$  transition (Figs. 11b–d). Thus, we conclude that the impact of the  $\text{NAO}^+$  to  $\text{ENAO}^-$  transition on the marked decline of the SAT seems to be confined to most of the European continent, while

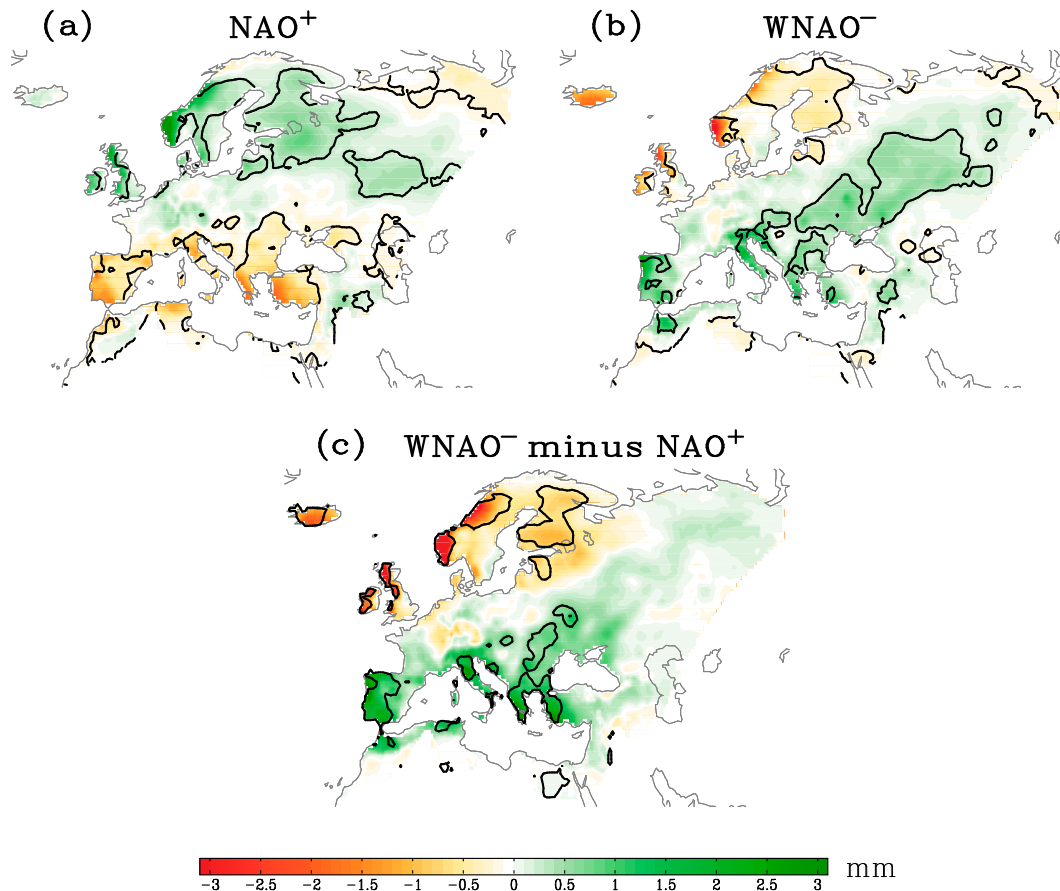


FIG. 10. As in Fig. 9, but for NAO<sup>+</sup> to WNAO<sup>-</sup> transition events (15 cases).

its impact on the precipitation is confined to southern Europe.

## 5. Composite in situ NAO events and their relationship with the variations of surface air temperature and precipitation anomalies

### a. Composite results of in situ NAO events

We show the composite SAT and precipitation anomalies (from lag -5 to lag +5 days) for in situ ENAO<sup>-</sup> and WNAO<sup>-</sup> events in Fig. 13. It is seen that the negative SAT anomaly occurs over a more widespread area for the in situ ENAO<sup>-</sup> regime (Fig. 13a) than for the in situ WNAO<sup>-</sup> regime (Fig. 13b), while confined mainly to central and northern Europe for the in situ WNAO<sup>-</sup> regime. A positive precipitation anomaly is seen over southwestern Europe and a small fraction of central Europe for the in situ ENAO<sup>-</sup> regime (Fig. 13c), and over southern Europe and the eastern part of central Europe for the in situ WNAO<sup>-</sup> regime (Fig. 13d). A comparison with Figs. 7 and 8 shows that the negative SAT anomaly is much stronger and occurs

over a more widespread area for the ENAO<sup>-</sup> regime of the NAO<sup>+</sup> to ENAO<sup>-</sup> transition event than for the in situ ENAO<sup>-</sup> regime, while their patterns look similar. In contrast, the strong negative SAT anomaly for the in situ WNAO<sup>-</sup> regime (Fig. 13b) is observed over a more widespread area than for the WNAO<sup>-</sup> regime (Fig. 8b) of the NAO<sup>+</sup> to WNAO<sup>-</sup> transition event. On the other hand, we can see that the change in the SAT anomaly between the in situ WNAO<sup>-</sup> and ENAO<sup>-</sup> regimes is not as notable as the difference between ENAO<sup>-</sup> and WNAO<sup>-</sup> regimes of the NAO<sup>+</sup> to ENAO<sup>-</sup> and NAO<sup>+</sup> to WNAO<sup>-</sup> transitions, as revealed in the next section. A similar result is also found for the precipitation anomaly pattern (Figs. 13c,d).

For a comparison, we show in Figs. 14 and 15 the temporal variation of the composite daily SAT and precipitation anomalies in the three subregions of Europe for the in situ ENAO<sup>-</sup> and WNAO<sup>-</sup> regimes. The two figures show that the variations of the SAT anomalies with the LW indices of in situ ENAO<sup>-</sup> and WNAO<sup>-</sup> events in the three European subregions are different from those of the NAO<sup>+</sup> to ENAO<sup>-</sup> and WNAO<sup>-</sup> transition events (Figs. 11 and 12).

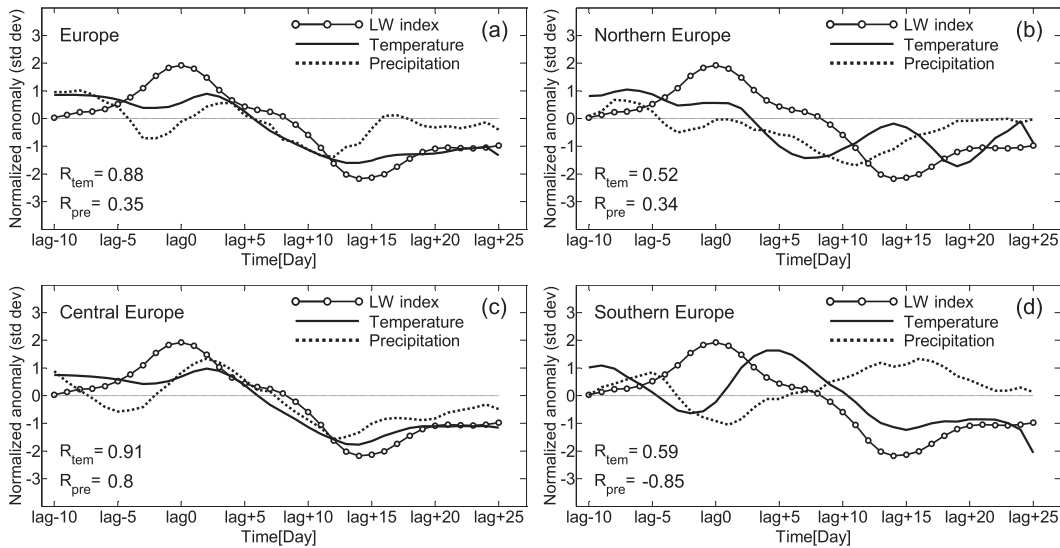


FIG. 11. Time series of the regional average SAT (solid) and precipitation (dotted) anomalies for the composite NAO<sup>+</sup> to ENAO<sup>-</sup> transition events (eight cases) over all of Europe and its three subregions: (a) all of Europe, (b) northern Europe, (c) central Europe, and (d) southern Europe, where lag 0 denotes the day with the largest NAO amplitude. A five-point smoothing is used for all the time series. Solid lines with dots represent the LW index for the NAO<sup>+</sup> to ENAO<sup>-</sup> transition event. In the panels,  $R_{\text{tem}}$  ( $R_{\text{pre}}$ ) represents the correlation coefficient between the LW index and the SAT (precipitation) anomaly time series in each region.

It is seen that the SAT anomaly over northern Europe exhibits a negative correlation of  $-0.41$  with the LW index for in situ ENAO<sup>-</sup> events (Fig. 14b), and a positive correlation of  $0.63$  for the in situ WNAO<sup>-</sup> events (Fig. 15b). In other words, there is a marked increase (decrease) of the SAT in northern Europe for in situ ENAO<sup>-</sup> (WNAO<sup>-</sup>) events. An interesting point is that the correlation between the SAT anomaly over central Europe and the LW index becomes positive for the in situ ENAO<sup>-</sup> (Fig. 14c) and WNAO<sup>-</sup> (Fig. 15c) events.

However, it is found that only the LW index for the in situ ENAO<sup>-</sup> events exhibits a significant positive correlation (a value of  $0.75$ ) with the SAT anomaly over southern Europe (Fig. 14d). Thus, the decline of the SAT occurs mainly over northern and central (northern, central, and southern) Europe for in situ WNAO<sup>-</sup> (ENAO<sup>-</sup>) events. However, a comparison with Fig. 11 clearly indicates that during the ENAO<sup>-</sup> period the decline of the SAT over central and southern Europe is more intense and persistent for the NAO<sup>+</sup> to ENAO<sup>-</sup>

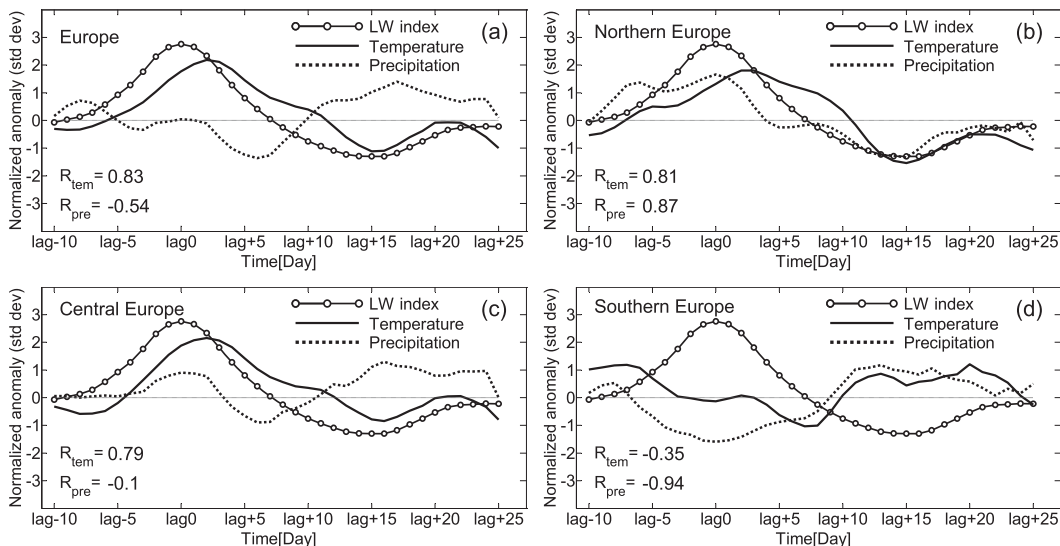


FIG. 12. As in Fig. 11, but for NAO<sup>+</sup> to WNAO<sup>-</sup> transition events (15 cases).

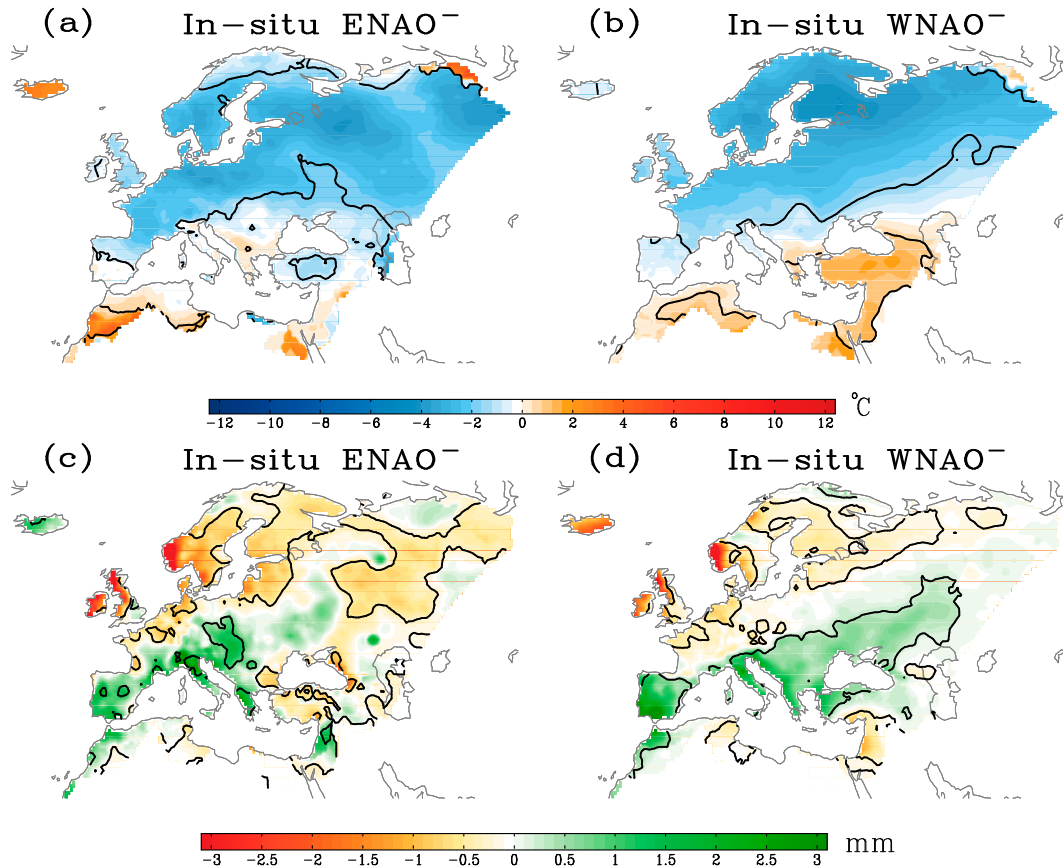


FIG. 13. Composites of the (a),(b) SAT anomalies and (c),(d) precipitation anomalies for (a),(c) in situ ENAO<sup>-</sup> (6 cases) and (b),(d) in situ WNAO<sup>-</sup> events (34 cases) during 1978–2012. The composite time interval is performed from lag -5 to lag +5 days, where lag 0 day denotes the day with the largest amplitude of the NAO anomaly. Solid lines denote the regions that exceed the 99% confidence level for a two-sided Student's *t* test.

transition events than for the in situ ENAO<sup>-</sup> events. Thus, the impact of the NAO<sup>+</sup> to ENAO<sup>-</sup> transition events on the variation of the SAT anomaly over central and southern Europe appears to be more important than that of in situ NAO<sup>-</sup> events. Also, the LW indices for in situ ENAO<sup>-</sup> and WNAO<sup>-</sup> events exhibit negative correlations of -0.63 and -0.88 with the precipitation anomaly over southern Europe (Figs. 14d and 15d), respectively, and positive correlations of 0.64 and 0.68, respectively, over northern Europe. Except over central Europe, the correlations are statistically significant at the 95% confidence level. One aspect of the in situ NAO<sup>-</sup> composite that differs from that of the NAO<sup>+</sup> to ENAO<sup>-</sup> transition is that the increase in the precipitation anomaly is mainly over southwestern Europe during the in situ NAO<sup>-</sup> period, but concentrated mostly over southern Europe during the ENAO<sup>-</sup> period of the NAO<sup>+</sup> to ENAO<sup>-</sup> transition. Although the impact of in situ ENAO<sup>-</sup> events on the SAT and precipitation anomalies is comparable to that of the ENAO<sup>-</sup> events of the NAO<sup>+</sup> to ENAO<sup>-</sup> transition, the

role of in situ ENAO<sup>-</sup> events is less important relative to that of the ENAO<sup>-</sup> events of the NAO<sup>+</sup> to ENAO<sup>-</sup> transition during 1978–2012 because the frequency of in situ ENAO<sup>-</sup> events is rather low and its impact is less persistent relative to the ENAO<sup>-</sup> events of the NAO<sup>+</sup> to ENAO<sup>-</sup> transition events.

From the above results, it is found that the decline of the composite SAT anomalies is more widespread and persistent for the ENAO<sup>-</sup> events of the NAO<sup>+</sup> to ENAO<sup>-</sup> transition than for those of the in situ ENAO<sup>-</sup> events. This may lead to extensive regions of colder weather over Europe, as observed in January–February 2012.

*b. A comparison between the composite surface air temperature and precipitation anomalies during negative phase episodes for in situ NAO and transition events*

To further see the contributions of different types of NAO<sup>-</sup> events to the variations of the SAT and precipitation anomalies, the differences of the composite SAT and precipitation anomalies between the in situ

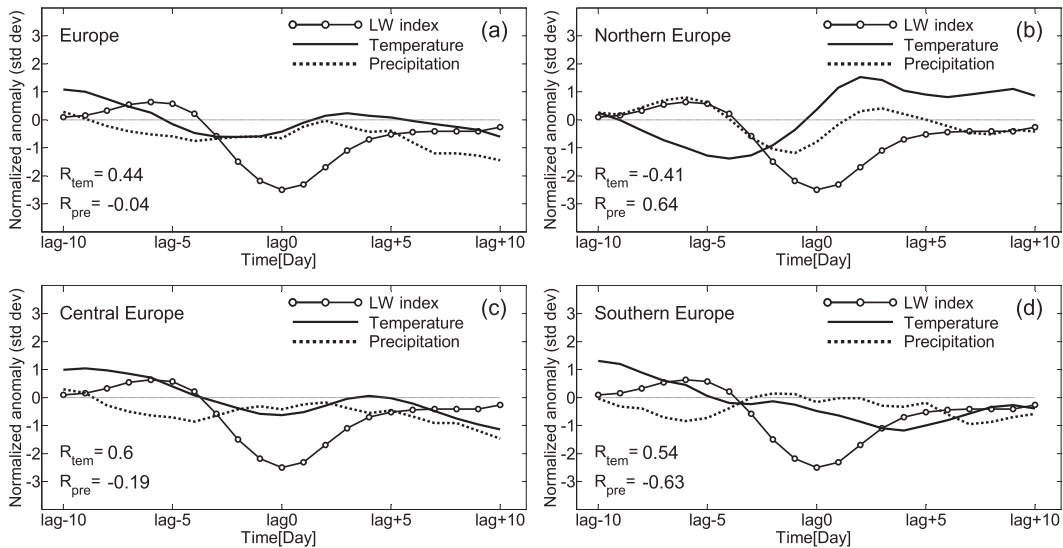


FIG. 14. Time series of the daily regional average SAT (solid) and precipitation (dotted) anomalies for the composite of in situ ENAO<sup>-</sup> events (six cases) over all of Europe and its three subregions: (a) all of Europe, (b) northern Europe, (c) central Europe, and (d) southern Europe. A five-point smoothing is used for all the time series. The solid line with dots represents the composite LW index for the in situ ENAO<sup>-</sup> events. In the panels,  $R_{\text{tem}}$  ( $R_{\text{pre}}$ ) represents the correlation coefficient between the composite LW index and the SAT (precipitation) anomaly time series in each region.

NAO<sup>-</sup> and NAO<sup>+</sup> to NAO<sup>-</sup> transition events (both for the ENAO<sup>-</sup> and WNAO<sup>-</sup>) are calculated. Figure 16a shows the difference of the composite SAT anomaly between the ENAO<sup>-</sup> and WNAO<sup>-</sup> events due to the NAO<sup>+</sup> to ENAO<sup>-</sup> and NAO<sup>+</sup> to WNAO<sup>-</sup> transitions, while the difference between in situ ENAO<sup>-</sup> and in situ WNAO<sup>-</sup> events is displayed in Fig. 16b. Moreover, we show in Fig. 16c the difference of the composite SAT anomaly between the ENAO<sup>-</sup> events due to the NAO<sup>+</sup> to ENAO<sup>-</sup> transition and in situ ENAO<sup>-</sup> events, and in

Fig. 16d the differences of the composite SAT anomaly between the WNAO<sup>-</sup> events due to the NAO<sup>+</sup> to WNAO<sup>-</sup> transition and in situ WNAO<sup>-</sup> events. Figures 16e–h show the corresponding composite precipitation anomaly differences as in Figs. 16a–d.

It is noted in Figs. 16a,b that the large negative value area of the composite SAT anomaly difference between ENAO<sup>-</sup> events due to the NAO<sup>+</sup> to ENAO<sup>-</sup> transitions and WNAO<sup>-</sup> events due to the NAO<sup>+</sup> to WNAO<sup>-</sup> transitions covers a much wider area than the

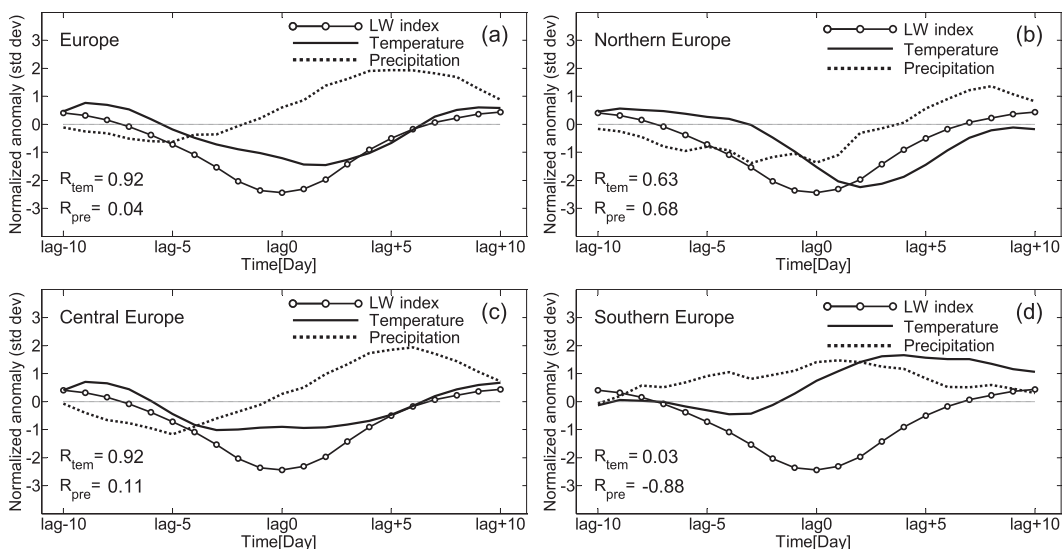


FIG. 15. As in Fig. 14, but for in situ WNAO<sup>-</sup> events (34 cases).

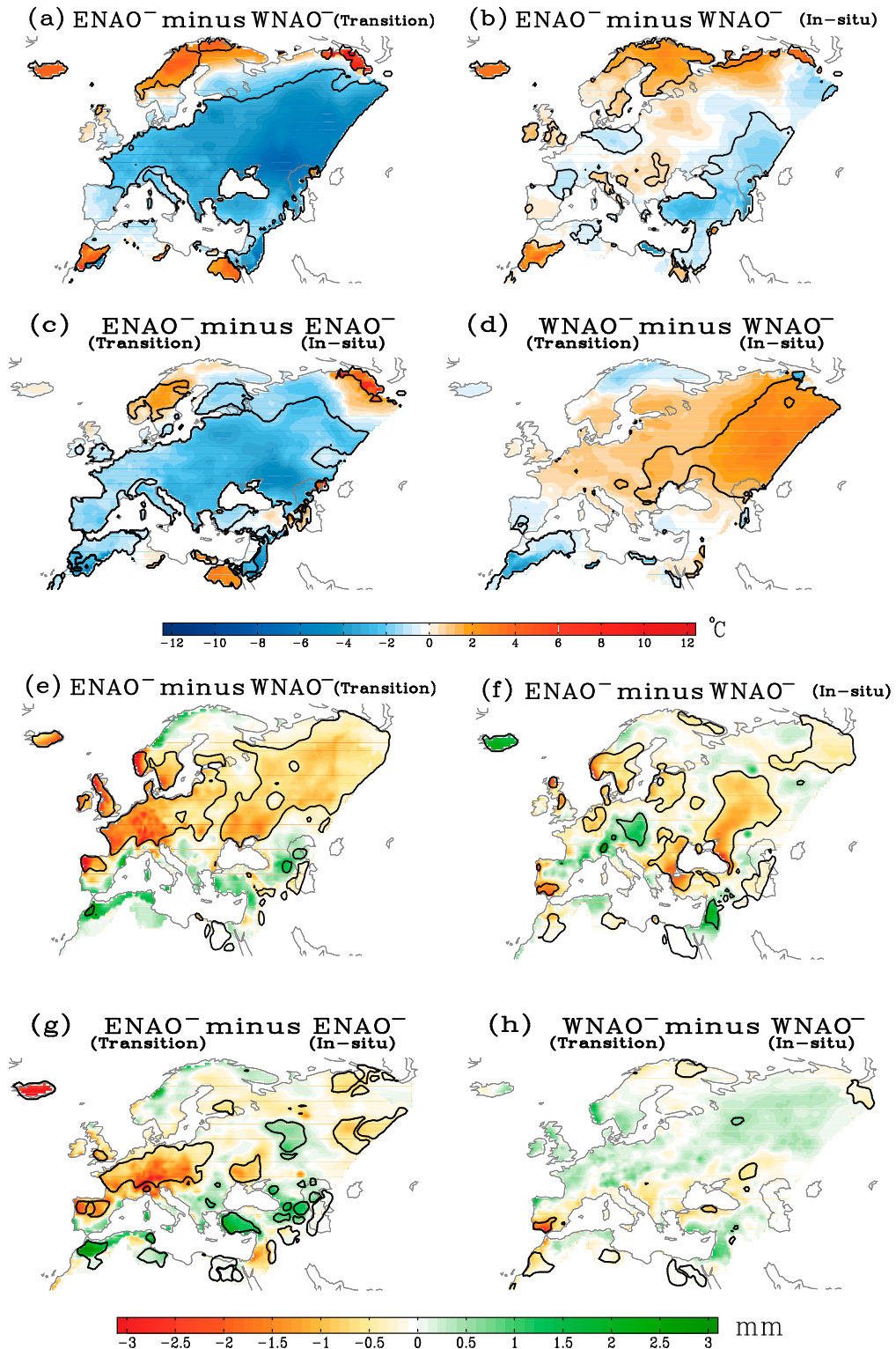


FIG. 16. The differences of the composite (a)–(d) SAT anomaly and (e)–(h) precipitation anomaly between (a),(e) the ENAO<sup>-</sup> and WNAO<sup>-</sup> (transition) events of the NAO<sup>+</sup> to ENAO<sup>-</sup> (8 cases) and NAO<sup>+</sup> to WNAO<sup>-</sup> transition events (15 cases); (b),(f) the in situ ENAO<sup>-</sup> (6 cases) and in situ WNAO<sup>-</sup> events (34 cases); (c),(g) the ENAO<sup>-</sup> (transition) events of the NAO<sup>+</sup> to ENAO<sup>-</sup> (8 cases) and in situ ENAO<sup>-</sup> (6 cases); and (d),(h) the WNAO<sup>-</sup> (transition) events of the NAO<sup>+</sup> to WNAO<sup>-</sup> (15 cases) and in situ WNAO<sup>-</sup> (34 cases). In the panels, solid lines denote the regions that exceed the 99% confidence level for a two-sided Student's *t* test.

difference between the in situ ENAO<sup>-</sup> and WNAO<sup>-</sup> events. Moreover, the strong negative area of the composite SAT anomaly difference between ENAO<sup>-</sup> events due to the NAO<sup>+</sup> to ENAO<sup>-</sup> transition and in situ ENAO<sup>-</sup> events also extends over a much larger area than that of the difference between WNAO<sup>-</sup> events due to the NAO<sup>+</sup> to WNAO<sup>-</sup> transition and in situ WNAO<sup>-</sup> events (Figs. 16c,d). Thus, the impact of the ENAO<sup>-</sup> event due to the NAO<sup>+</sup> to ENAO<sup>-</sup> transition on the SAT decline is much stronger and mainly concentrated in the southern part of northern Europe, central Europe, and most of southern Europe (Figs. 16a and 16c). In contrast, the impact of other types of NAO<sup>-</sup> events on the SAT decrease is relatively weak and mainly located in a narrower region (Figs. 16b,d). On the other hand, we can see from Figs. 16e–h that during the ENAO<sup>-</sup> period of the NAO<sup>+</sup> to ENAO<sup>-</sup> transition event the dominant positive precipitation anomaly occurs mainly in southern Europe and a small part of the positive precipitation anomaly is located in northernmost Europe. In particular, the difference of the composite precipitation anomaly between ENAO<sup>-</sup> events due to the NAO<sup>+</sup> to ENAO<sup>-</sup> transitions and in situ ENAO<sup>-</sup> events over southern Europe is significant at the 95% confidence level for a two-sided Student's *t* test (Fig. 16g). Thus, it is thought that the NAO<sup>+</sup> to ENAO<sup>-</sup> transition event is a most important contributor to the marked decline of the SAT over the European continent, leading to a severe cold wave over Eurasian continent as observed in January–February 2012. A similar result is also found for the case when the NAO<sup>-</sup> pattern is located to the east (west) of 20°W, corresponding to the definition of the ENAO<sup>-</sup> (WNAO<sup>-</sup>) pattern (not shown).

Here, we discuss why the NAO<sup>+</sup> to ENAO<sup>-</sup> transition events lead to colder conditions than other NAO<sup>-</sup> events. As suggested by Sillmann et al. (2011), blocking events over the western North Atlantic seem to have less influence on temperatures in Europe than do blocking events closer to the continent. Because in situ WNAO<sup>-</sup> (North Atlantic blocking) events are far from the European continent, the impact of in situ WNAO<sup>-</sup> events on the decrease of the SAT over the European continent is not more important than that of in situ ENAO<sup>-</sup> (European blocking) events even though the composite LW index of in situ WNAO<sup>-</sup> events are negatively stronger and more persistent than that of in situ ENAO<sup>-</sup> events (Fig. 6d). This difference can also be seen from a comparison between Figs. 16b and 16d. Moreover, because the ENAO<sup>-</sup> events due to the NAO<sup>+</sup> to ENAO<sup>-</sup> transitions are long lived (Fig. 6c) and in situ ENAO<sup>-</sup> events are relatively short lived (Fig. 6d), the impact of ENAO<sup>-</sup> events associated with the NAO<sup>+</sup> to ENAO<sup>-</sup> transitions on the decline of the

SAT over Europe is more intense and persistent than in situ ENAO<sup>-</sup> events. On the other hand, the composite amplitude of ENAO<sup>-</sup> events for the NAO<sup>+</sup> to ENAO<sup>-</sup> transition events is stronger than that of WNAO<sup>-</sup> events for the NAO<sup>+</sup> to WNAO<sup>-</sup> transition events, as shown in Fig. 6c. As a result, the decline of the SAT over Europe is more intense due to the impact of ENAO<sup>-</sup> events associated with the NAO<sup>+</sup> to ENAO<sup>-</sup> transition than due to that of WNAO<sup>-</sup> events associated with the NAO<sup>+</sup> to WNAO<sup>-</sup> transition. Thus, the present study suggests that this type of large-scale regime transition is generally favorable for wintertime cold air outbreaks over Europe.

## 6. Conclusions and discussion

In this paper, we have investigated the possible cause of the outbreak of the extreme cold weather event over Europe that took place in January–February 2012. It is found that the outbreak of the extreme cold event over the European continent in January–February 2012 is closely related to the transition from a NAO<sup>+</sup> event to a long-lasting ENAO<sup>-</sup> (an eastern Atlantic–European blocking) event. Before the NAO transition began on 21 January, a single Atlantic–European storm track was observed over central Europe. The Atlantic storm tracks split into two branches over the European continent as the NAO<sup>+</sup> event evolved into an ENAO<sup>-</sup> event. Because the ENAO<sup>-</sup> event was long lived during the period from 21 January to 13 February 2012, the double storm track persisted for the same time over the European continent because the double storm track and the ENAO<sup>-</sup> pattern tend to have the same time scale (Luo et al. 2007). The presence of the persistent double storm track appears to maintain a persistent anomalously low SAT over most of Europe as well as a persistent increase in precipitation (including snow) over southern Europe. Thus, the case study provides a likely explanation for the outbreak of the extreme cold event over the European continent observed in January–February 2012.

A statistical analysis based upon the LW index shows that ENAO<sup>-</sup> events of the NAO<sup>+</sup> to ENAO<sup>-</sup> transition are more frequent and intense during 2005–12 than WNAO<sup>-</sup> events of the NAO<sup>+</sup> to WNAO<sup>-</sup> transition. Composites of SAT and precipitation anomalies for NAO<sup>+</sup> to ENAO<sup>-</sup> and WNAO<sup>-</sup> transition events and in situ ENAO<sup>-</sup> and WNAO<sup>-</sup> events are performed. It is found that the composite SAT and precipitation anomaly patterns for NAO<sup>+</sup> to ENAO<sup>-</sup> transition events are noticeably different from those for NAO<sup>+</sup> to WNAO<sup>-</sup> transition events and in situ ENAO<sup>-</sup> and WNAO<sup>-</sup> events. The negative SAT anomalies are concentrated over all of Europe (northern and central

Europe) as the  $\text{NAO}^+$  pattern transitions into the  $\text{ENAO}^-$  ( $\text{WNAO}^-$ ) pattern. It is also shown that for the  $\text{NAO}^+$  to  $\text{NAO}^-$  transition events the decline of the SAT is more persistent for the  $\text{ENAO}^-$  pattern than for the  $\text{WNAO}^-$  pattern because the  $\text{ENAO}^-$  anomaly is stronger than the  $\text{WNAO}^-$  anomaly. Moreover, a comparison with in situ  $\text{ENAO}^-$  and  $\text{WNAO}^-$  events is also made. It is found that the impact of the  $\text{NAO}^+$  to  $\text{ENAO}^-$  transition events on the decline of the SAT over Europe is more persistent and occurs over a wider region than in situ  $\text{ENAO}^-$  and  $\text{WNAO}^-$  events. Thus, the present study suggests that the  $\text{NAO}^+$  to  $\text{ENAO}^-$  transitions may be favorable for cold air outbreaks over Europe. The impact of the  $\text{NAO}^+$  to  $\text{ENAO}^-$  transition event on the decline of surface air temperature is especially strong and persistent over central and southern Europe.

In this study, although we have linked the European extreme cold event in January–February 2012, and that of recent winters, to the  $\text{NAO}^+$  to  $\text{ENAO}^-$  transition events, the physical mechanism of the  $\text{NAO}^+$  to  $\text{ENAO}^-$  transition events is not examined in detail. In addition, we do not distinguish the difference between  $\text{NAO}^-$  and blocking events. Instead, Atlantic and eastern Atlantic–European blocking events are defined as  $\text{WNAO}^-$  and  $\text{ENAO}^-$  events, respectively, even though their dynamical processes may be different. Such a definition of the  $\text{ENAO}^-$  and  $\text{WNAO}^-$  regimes may also reflect eastward- and westward-displaced  $\text{NAO}^-$  patterns (Johnson et al. 2008). On the other hand, the classification of the  $\text{NAO}^+$  to  $\text{NAO}^-$  transitions into  $\text{NAO}^+$  to  $\text{WNAO}^-$  (Atlantic blocking) and  $\text{NAO}^+$  to  $\text{ENAO}^-$  (eastern Atlantic–European blocking) transitions can help us to better understand how the zonal position of  $\text{NAO}^-$  regimes associated with the  $\text{NAO}^+$  to  $\text{NAO}^-$  transition affects cold air outbreaks over Europe.

In this paper, we did not focus our attention on the difference in the dynamics between in situ  $\text{NAO}^-$  events and eastern Atlantic–European blocking ( $\text{ENAO}^-$ ) regimes associated with the  $\text{NAO}^+$  to  $\text{ENAO}^-$  transitions. Instead, the emphasis of our study was on large-scale aspects of cold air outbreaks over Europe. However, some investigations have revealed that the classification of  $\text{NAO}^-$  (blocking) events into Atlantic blocking and eastern Atlantic–European blocking events, defined as  $\text{WNAO}^-$  and  $\text{ENAO}^-$  events, respectively, has at least a dynamical and observational basis (Luo et al. 2011; Michel and Rivière 2011; Sung et al. 2011; Luo and Cha 2012). The number of  $\text{NAO}^+$  to eastern Atlantic–European blocking ( $\text{ENAO}^-$ ) transition events is underestimated if the regime definition of the PC index is used (not shown). However, the use of the LW index can increase the number of  $\text{NAO}^+$  to  $\text{ENAO}^-$  transition events because it can better capture the  $\text{NAO}^+$  to

eastern Atlantic–European blocking regime ( $\text{ENAO}^-$ ) transition.

It should be noted that in this paper we did not examine the roles of the east Atlantic pattern (EA; Wallace and Gutzler 1981) and the strong persistent ridge episode (SPRE; Santos et al. 2009; Woollings et al. 2011; Santos et al. 2013) in cold air outbreaks over Europe. Instead, we have emphasized in particular the role of the  $\text{NAO}^+$  to  $\text{ENAO}^-$  transition events in the outbreak of cold waves over the European continent by considering the different positions of the  $\text{NAO}^-$  events associated with the  $\text{NAO}^+$  to  $\text{NAO}^-$  transitions. A recent study also revealed that extreme cold events over Europe may be related to the EA pattern, although the EA is the second EOF mode of the geopotential height field in the Euro–Atlantic sector (Moore and Renfrew 2012). Even so, the different roles of the NAO, EA, and SPRE in the occurrence of European extreme cold events deserve further investigation. On the other hand, the physical process of how the storm track affects the variations of the SAT and precipitation anomaly patterns during NAO episodes was not examined from a synoptic perspective, although the variations of the SAT and precipitation anomalies in mid- to high latitudes can in part be explained in terms of the different strengths and positions of transient synoptic-scale cyclones (Archambault et al. 2010). Further diagnostic study on the synoptic processes associated with the cold wave over the European continent in January–February 2012 is needed in the future.

Recent studies have also revealed that European extreme cold weather is closely related to the decrease of the summer Arctic sea ice extent (Liu et al. 2012). This implies that different cold waves over Europe might have different physical processes. But, in the present study we only emphasized the role of the NAO regime change in extreme cold events over Europe. Even so, the present study provides useful evidence that  $\text{NAO}^+$  to  $\text{ENAO}^-$  transition events are favorable for European extreme cold events.

*Acknowledgments.* The authors acknowledge the support from the National Science Foundation of China (Grants 41375067 and 41430533), the “One Hundred Talent Plan” of the Chinese Academy of Sciences (Grant Y163011), and National Science Foundation Grants AGS-1036858 and AGS-1401220. The authors thank three anonymous reviewers for their constructive suggestions in improving this paper.

## REFERENCES

- Archambault, H. M., D. Keyser, and L. F. Bosart, 2010: Relationship between large-scale regime transitions and major

- cool-season precipitation events in the northeastern United States. *Mon. Wea. Rev.*, **138**, 3454–3473, doi:10.1175/2010MWR3362.1.
- Benedict, J. J., S. Lee, and S. B. Feldstein, 2004: Synoptic view of the North Atlantic Oscillation. *J. Atmos. Sci.*, **61**, 121–144, doi:10.1175/1520-0469(2004)061<0121:SVOTNA>2.0.CO;2.
- Buehler, T., C. C. Raible, and T. F. Stocker, 2011: The relationship of winter season North Atlantic blocking frequency to extreme cold or dry spells in the ERA-40. *Tellus*, **63A**, 212–222, doi:10.1111/j.1600-0870.2010.00492.x.
- Cai, M., and M. Mak, 1990: Symbiotic relation between planetary and synoptic-scale waves. *J. Atmos. Sci.*, **47**, 2953–2968, doi:10.1175/1520-0469(1990)047<2953:SRBPAS>2.0.CO;2.
- Cattiaux, J., R. Vautard, C. Cassou, P. Yiou, V. Masson-Delmotte, and F. Codron, 2010: Winter 2010 in Europe: A cold extreme in a warming climate. *Geophys. Res. Lett.*, **37**, L20704, doi:10.1029/2010GL044613.
- Croci-Maspoli, M., and H. C. Davies, 2009: Key dynamical features of the 2005/06 European winter. *Mon. Wea. Rev.*, **137**, 644–678, doi:10.1175/2008MWR2533.1.
- Davini, P., C. Cagnazzo, R. Neale, and J. Tribbia, 2012: Coupling between Greenland blocking and the North Atlantic Oscillation pattern. *Geophys. Res. Lett.*, **39**, L14701, doi:10.1029/2012GL052315.
- De Vries, H., R. J. Haarsma, and W. Hazeleger, 2012: Western European cold spells in current and future climate. *Geophys. Res. Lett.*, **39**, L04706, doi:10.1029/2011GL050665.
- Feldstein, S. B., 2003: The dynamics of NAO teleconnection pattern growth and decay. *Quart. J. Roy. Meteor. Soc.*, **129**, 901–924, doi:10.1256/qj.02.76.
- Glahn, H. R., 1968: Canonical correlation and its relationship to discriminant analysis and multiple regressions. *J. Atmos. Sci.*, **25**, 23–31, doi:10.1175/1520-0469(1968)025<0023:CCAIRT>2.0.CO;2.
- Hamming, R. W., 1989: *Digital Filters*. Prentice-Hall, 284 pp.
- Hurrell, J. W., 1995: Decadal trends in the North Atlantic Oscillation: Regional temperature and precipitation. *Science*, **269**, 676–679, doi:10.1126/science.269.5224.676.
- , and H. van Loon, 1997: Decadal variations in climate associated with the North Atlantic Oscillation. *Climate Change*, **36**, 301–336, doi:10.1023/A:1005314315270.
- Johnson, N. C., S. B. Feldstein, and B. Trembley, 2008: The continuum of Northern Hemisphere teleconnection patterns and a description of the NAO shift with the use of self-organizing maps. *J. Climate*, **21**, 6354–6371, doi:10.1175/2008JCLI2380.1.
- Li, J., and X. L. Wang, 2003: A new North Atlantic oscillation index and its variability. *Adv. Atmos. Sci.*, **20**, 661–676, doi:10.1007/BF02915394.
- Liu, J., J. A. Curry, H. Wang, M. Song, and R. M. Horton, 2012: Impact of declining Arctic sea ice on winter snowfall. *Proc. Natl. Acad. Sci. USA*, **109**, 4074–4079, doi:10.1073/pnas.1114910109.
- Livezey, R. E., and W. Y. Chen, 1983: Statistical field significance and its determination by Monte Carlo techniques. *Mon. Wea. Rev.*, **111**, 46–59, doi:10.1175/1520-0493(1983)111<0046:SFSAID>2.0.CO;2.
- Luo, D., 2005: A barotropic envelope Rossby soliton model for block–eddy interaction. Part I: Effect of topography. *J. Atmos. Sci.*, **62**, 5–21, doi:10.1175/1186.1.
- , and J. Cha, 2012: The North Atlantic Oscillation and North Atlantic jet variability: Precursors to NAO regimes and transitions. *J. Atmos. Sci.*, **69**, 3763–3787, doi:10.1175/JAS-D-12-098.1.
- , A. Lupo, and H. Wan, 2007: Dynamics of eddy-driven low-frequency dipole modes. Part I: A simple model of North Atlantic Oscillations. *J. Atmos. Sci.*, **64**, 3–38, doi:10.1175/JAS3818.1.
- , Y. Diao, and S. B. Feldstein, 2011: The variability of the Atlantic storm track and the North Atlantic Oscillation: A link between intraseasonal and interannual variability. *J. Atmos. Sci.*, **68**, 577–601, doi:10.1175/2010JAS3579.1.
- , J. Cha, and S. B. Feldstein, 2012a: Weather regime transitions and the interannual variability of the North Atlantic Oscillation. Part I: A likely connection. *J. Atmos. Sci.*, **69**, 2329–2346, doi:10.1175/JAS-D-11-0289.1.
- , —, and —, 2012b: Weather regime transitions and the interannual variability of the North Atlantic Oscillation. Part II: Dynamical processes. *J. Atmos. Sci.*, **69**, 2347–2363, doi:10.1175/JAS-D-11-0290.1.
- Michel, C., and G. Rivière, 2011: The link between Rossby wave breakings and weather regime transitions. *J. Atmos. Sci.*, **68**, 1730–1748, doi:10.1175/2011JAS3635.1.
- Moore, G. W. K., and I. A. Renfrew, 2012: Cold European winters: Interplay between the NAO and the East Atlantic mode. *Atmos. Sci. Lett.*, **13**, 1–8, doi:10.1002/asl.356.
- Pfahl, S., and H. Wernli, 2012: Quantifying the relevance of atmospheric blocking for co-located temperature extremes in the Northern Hemisphere on (sub-) daily time scales. *Geophys. Res. Lett.*, **39**, L12807, doi:10.1029/2012GL052261.
- Santos, J. A., J. G. Pinto, and U. Ulbrich, 2009: On the development of strong ridge episodes over the eastern North Atlantic. *Geophys. Res. Lett.*, **36**, L17804, doi:10.1029/2009GL039086.
- , T. Woollings, and J. G. Pinto, 2013: Are the winters 2010 and 2012 archetypes exhibiting extreme opposite behavior of the North Atlantic jet stream? *Mon. Wea. Rev.*, **141**, 3626–3640, doi:10.1175/MWR-D-13-00024.1.
- Scaife, A. A., C. K. Folland, L. V. Alexander, A. Moberg, and J. R. Knight, 2008: European climate extremes and the North Atlantic Oscillation. *J. Climate*, **21**, 72–83, doi:10.1175/2007JCLI1631.1.
- Seager, R., Y. Kushnir, J. Nakamura, M. Ting, and N. Naik, 2010: Northern Hemisphere winter snow anomalies: ENSO, NAO and the winter of 2009/10. *Geophys. Res. Lett.*, **37**, L14703, doi:10.1029/2010GL043830.
- Shabbar, A., J. Huang, and K. Higuchi, 2001: The relationship between the wintertime North Atlantic Oscillation and blocking episodes in the North Atlantic. *Int. J. Climatol.*, **21**, 355–369, doi:10.1002/joc.612.
- Sillmann, J., M. Croci-Maspoli, M. Kallache, and R. W. Katz, 2011: Extreme cold winter temperatures in Europe under the influence of North Atlantic atmospheric blocking. *J. Climate*, **24**, 5899–5913, doi:10.1175/2011JCLI4075.1.
- Sisson, P. A., and J. R. Gyakum, 2004: Synoptic-scale precursors to significant cold-season precipitation events in Burlington, Vermont. *Wea. Forecasting*, **19**, 841–854, doi:10.1175/1520-0434(2004)019<0841:SPTSCP>2.0.CO;2.
- Sung, M.-K., G.-H. Lim, J.-S. Kug, and S.-I. An, 2011: A linkage between the North Atlantic Oscillation and its downstream development due to the existence of a blocking ridge. *J. Geophys. Res.*, **116**, D11107, doi:10.1029/2010JD015006.
- Vicente-Serrano, S. M., and J. I. López-Moreno, 2008: Non-stationary influence of the North Atlantic Oscillation on European precipitation. *J. Geophys. Res.*, **113**, D20120, doi:10.1029/2008JD010382.
- Wallace, J. M., and D. S. Gutzler, 1981: Teleconnections in the geopotential height field during the Northern Hemisphere winter. *Mon. Wea. Rev.*, **109**, 784–812, doi:10.1175/1520-0493(1981)109<0784:TITGHF>2.0.CO;2.

- Wang, C., H. Liu, and S.-K. Lee, 2010: The record-breaking cold temperatures during the winter of 2009/2010 in the Northern Hemisphere. *Atmos. Sci. Lett.*, **11**, 161–168, doi:[10.1002/asl.278](https://doi.org/10.1002/asl.278).
- Werner, P. C., F. W. Gerstengarbe, K. Fraedrich, and H. Oesterle, 2000: Recent climate change in the North Atlantic European sector. *Int. J. Climatol.*, **20**, 463–471, doi:[10.1002/\(SICI\)1097-0088\(200004\)20:5<463::AID-JOC483>3.0.CO;2-T](https://doi.org/10.1002/(SICI)1097-0088(200004)20:5<463::AID-JOC483>3.0.CO;2-T).
- Woollings, T., B. J. Hoskins, M. Blackburn, and P. Berrisford, 2008: A new Rossby wave-breaking interpretation of the North Atlantic Oscillation. *J. Atmos. Sci.*, **65**, 609–626, doi:[10.1175/2007JAS2347.1](https://doi.org/10.1175/2007JAS2347.1).
- , J. G. Pinto, and J. A. Santos, 2011: Dynamical evolution of North Atlantic ridges and poleward jet stream displacements. *J. Atmos. Sci.*, **68**, 954–963, doi:[10.1175/2011JAS3661.1](https://doi.org/10.1175/2011JAS3661.1).
- Yiou, P., and M. Nogaj, 2004: Extreme climate events and weather regimes over the North Atlantic: When and where? *Geophys. Res. Lett.*, **31**, L07202, doi:[10.1029/2003GL019119](https://doi.org/10.1029/2003GL019119).
- Zhang, X., C. Lu, and Z. Guan, 2012: Weakened cyclones, intensified anticyclones and recent extreme cold winter weather events in Eurasia. *Environ. Res. Lett.*, **7**, 044044, doi:[10.1088/1748-9326/7/4/044044](https://doi.org/10.1088/1748-9326/7/4/044044).
- Zhou, W., J. C. L. Chan, W. Chen, J. Ling, J. G. Pinto, and Y. Shao, 2009: Synoptic-scale controls of persistent low temperature and icy weather over southern China in January 2008. *Mon. Wea. Rev.*, **137**, 3978–3991, doi:[10.1175/2009MWR2952.1](https://doi.org/10.1175/2009MWR2952.1).